Physics & diagnostics in Tokamak plasmas
-
Plasma equilibrium

Cyrille Honoré cyrille.honore@polytechnique.edu
Laboratoire de Physique des Plasmas
CNRS – Sorb. Univ. – UPSaclay – ObsParis,
École Polytechnique – IP Paris
91128 Palaiseau cedex, France

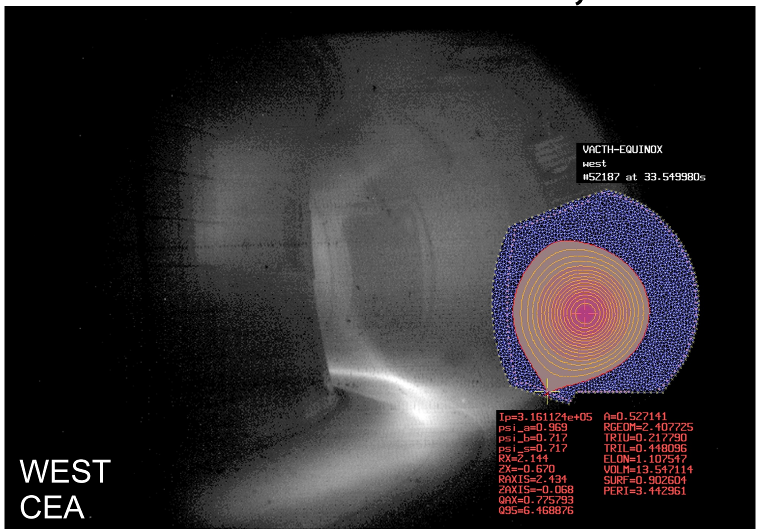

Physics and Diagnostics in Tokamak plasmas

How do we control Tokamak plasma **equilibrium** ?
How do we run a Tokamak **shot** ?
How do we control plasma **MHD instabilities** ?
How do we check the plasma **confinement** ?
How do we check the plasma performance **(density and temperature)** ?
How do we control plasma **impurities** dynamics (any particle different as D and T) ?
How do we control **high energy particles** ?
How do control **plasma wall interaction** ?
How do we observe plasma **micro-turbulence** that reduces plasma confinement ?
What can we do to enhance the **plasma confinement** ?
…

Physics and Diagnostics in Tokamak plasmas

PPF – E2
GI-PLATO – FM2

- **I. MHD equilibrium,** C. Honoré, Fri 5/12 2PM
- **II. Tokamak MHD stability,** P. Morel, Fri 12/12 9AM
- **III. Thomson Scattering,** C. Honoré, Fri 19/12 2PM
- **IV. Spectroscopy 1,** R. Guirlet, Fri 16/01 9AM
- **V. Spectroscopy 2,** R. Guirlet, Fri 16/01 2PM
- **VI. Kinetic profiles,** P. Morel, Fri 23/01 9AM
- **VII. Edge flows and turbulence,** P. Morel, Fri 30/01 9AM
- **VIII. Core turbulence,** C. Honoré, Fri 30/01 2PM

- **Articles to be presented by 2 (or 3) students** (Mon 9/02 AM & PM)

- **Short exam (1h30 - 2h)** (Fri 13/02, 2PM)

Lecture

- I. Magneto-Hydro-Dynamics equilibrium
  - Tokamak plasma equilibrium
    - Kinetic and magnetic pressure balance
    - Tokamak equilibrium comprehensive description
    - Simplest circular tokamak equilibrium
    - Tokamak plasma control and shaping
  - Plasma shot scenarios
  - Equilibrium diagnostics
    - Magnetic measurements
    - Interferometry
    - Polarimetry
  - MHD equilibrium reconstruction

Tokamak plasma equilibrium

Stationary MHD equations

Ideal MHD equilibrium equations :

- Force balance (Laplace and pressure forces): $\vec{j} \wedge \vec{B} = \vec{\nabla} P$
- Maxwell-Ampere equation: $\vec{\nabla} \wedge \vec{B} = \mu_0 \vec{j}$
- Maxwell-Thomson equation: $\nabla . \vec{B} = 0$

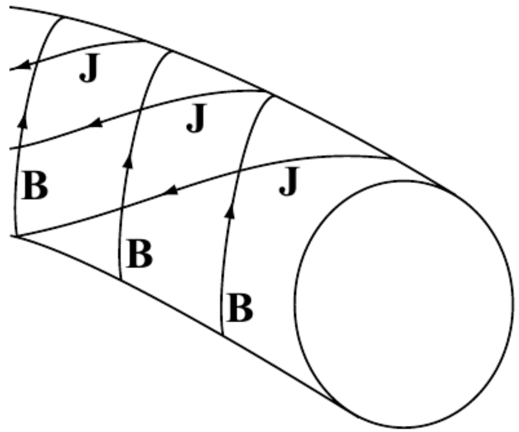

J. Freidberg

Magnetic flux surfaces

Force balance equation $\vec{j} \wedge \vec{B} = \vec{\nabla} P$ implies :

$$\vec{j} . \vec{\nabla} P = 0$$

$$\vec{B} . \vec{\nabla} P = 0$$

Pressure is constant on **flux surfaces** defined by magnetic lines and electric currents.

Pressure gradient is present only when magnetic lines and currents are not co-linear.

Tokamak plasma Equilibrium

The tokamak plasma MHD equilibrium is made with **magnetic flux tores** inside one another.

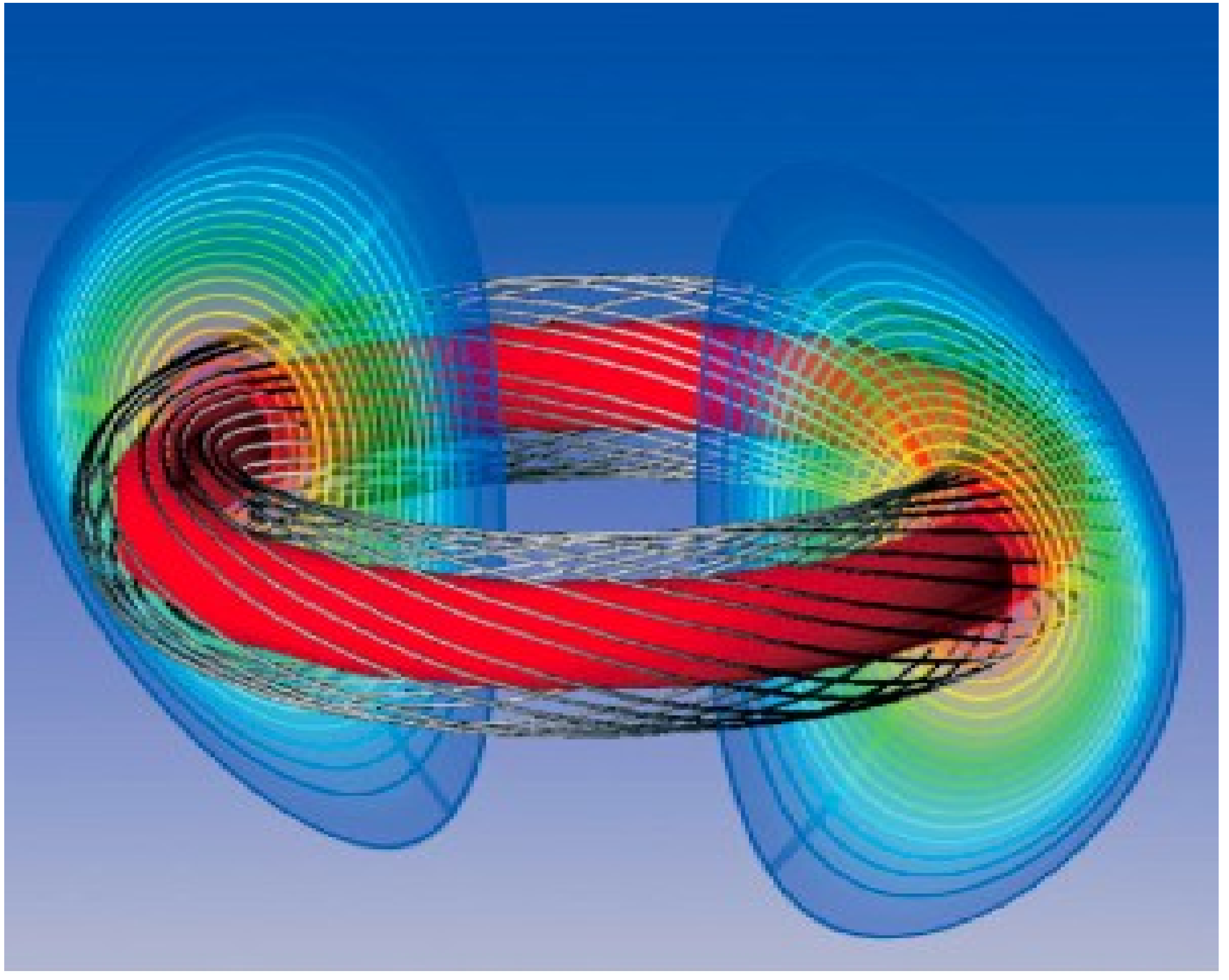

Magnetic and kinetic pressure balance

Maxwell-Ampere equation : $\vec{\nabla} \wedge \vec{B} = \mu_0 \vec{j}$

Is used to eliminate the current in the momentum conservation equation : $\vec{j} \wedge \vec{B} = \vec{\nabla} P$

$$\frac{1}{\mu_0} (\vec{\nabla} \wedge \vec{B}) \wedge \vec{B} = \vec{\nabla} P$$

Using the gradient property :

$$\vec{\nabla} \left(\frac{B^2}{2} \right) = \vec{B} \wedge (\vec{\nabla} \wedge \vec{B}) + (\vec{B} . \vec{\nabla}) \vec{B}$$

We get pressure balance relation :

$$\boxed{\vec{\nabla}_{\perp} \left(P + \frac{B^2}{2\mu_0} \right) - \frac{B^2}{\mu_0} \frac{1}{R_B} \vec{e}_n = 0}$$

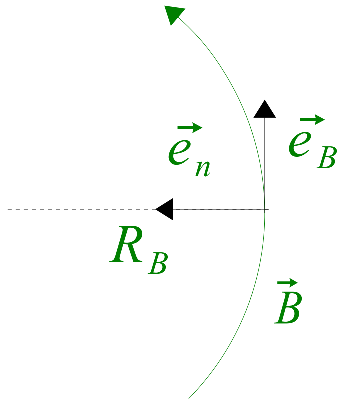

where $\vec{e}_n$ is the magnetic field line curvature direction.

$\vec{e}_B$ is the magnetic field direction : $\vec{e}_B = \frac{1}{B} \vec{B}$

R_B is the magnetic field line curvature radius

$\vec{\nabla}_{\parallel}$ is the gradient component parallel to the magnetic field $\vec{B}$:

$$\vec{\nabla}_{\parallel} = \vec{e}_B (\vec{e}_B . \vec{\nabla})$$

$\vec{\nabla}_{\perp}$ is the gradient complementary component, for the perpendicular direction:

$$\vec{\nabla}_{\perp} = \vec{\nabla} - \vec{e}_B (\vec{e}_B . \vec{\nabla})$$

Kinetic and magnetic pressure ratio

Pressure balance : $$\vec{\nabla}_{\perp}\left(P+\frac{B^2}{2\mu_0}\right)-\frac{B^2}{2\mu_0}\frac{1}{R_B}\vec{e}_n=0$$

This relation shows a balance between the kinetic pressure P and the complementary magnetic pressure :

$$P_B=\frac{B^2}{2\mu_0}$$

The additional term of the pressure balance equation is the tension induced by the magnetic field line curvature : $$-\frac{B^2}{2\mu_0}\frac{1}{R_B}\vec{e}_n$$

We suppose the magnetic field line curvature is negligible:
Following a direction perpendicular to $\vec{B}$ towards plasma edge.
At the plasma edge : $B=B_a$, $P=0$
Between a position inside the plasma and the plasma edge : $P+\frac{B^2}{2\mu_0}=\frac{B_a^2}{2\mu_0}$

This implies : $P\leq\frac{B_a^2}{2\mu_0}$

The kinetic pressure inside is always smaller than the magnetic pressure at the edge (not taking the curvature effects into account).
We define β a dimensionless quantity comparing the the kinetic to the magnetic pressure :

$$\beta=\frac{2\mu_0 P}{B^2}$$

1D equilibrium : the θ pinch

The geometry is cylindrical.
The magnetic field is axial : $\vec{B} = B_z(r)\vec{e}_z$
Azimuthal current : $\vec{j} = j_\theta(r)\vec{e}_\theta$
Field and current vary radially.

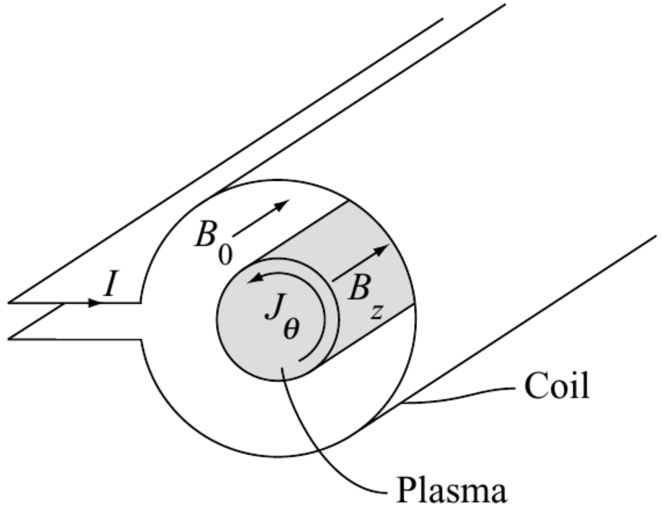

Maxwell-Ampere law $\vec{\nabla} \wedge \vec{B} = \mu_0 \vec{j}$ implies :

$$\frac{d B_z}{d r} = -\mu_0 j_\theta$$

The magnetic field decreases radially.
Since the magnetic field is not curved :

$$\frac{d}{d r}\left(P + \frac{B_z^2}{2\mu_0}\right) = 0$$

The kinetic pressure increases towards the axis.
B_{za} is the magnetic field outside the plasma ($P(a)=0$) :

$$P(r) = \frac{B_{za}^2 - B_z(r)^2}{2\mu_0}$$

The kinetic pressure is always below the magnetic pressure outside the plasma.

$$B_z(r) < B_{za}$$

Because of the kinetic pressure, **the magnetic field is reduced inside the plasma**.
The plasma pressure has a **diamagnetic** effect.

2D equilibrium for a tore : the kinetic pressure

The **tore surface** for a given large radius R_0 and small radius r , is smaller for the inside than for the outside parts :

$$S_{\text{lfs}} = \int_0^{2\pi} d\phi \int_{-\pi/2}^{\pi/2} d\theta \, R\, r$$

$$S_{\text{lfs}} = 2\pi \int_{-\pi/2}^{\pi/2} (R_0 + r\cos\theta)\, r\, d\theta \qquad R = R_0 + r\cos\theta$$

$$S_{\text{lfs}} = 2\pi r (\pi R_0 + 2r)$$

$$S_{\text{hfs}} = 2\pi \int_{-\pi/2}^{\pi/2} (R_0 - r\cos\theta)\, r\, d\theta \qquad R = R_0 - r\cos\theta$$

$$S_{\text{hfs}} = 2\pi r (\pi R_0 - 2r) \leq S_{lfs}$$

Poloidal section

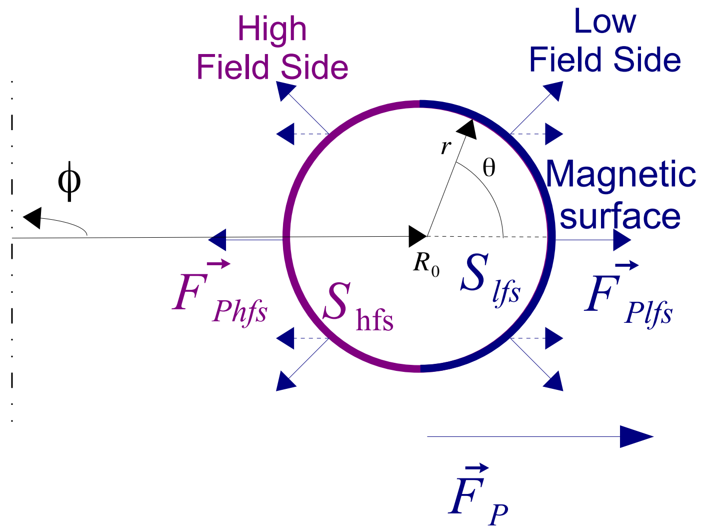

The **kinetic pressure** is oriented outwards the plasma.
The vertical force is null due to the tore vertical symmetry
The pressure radial component is different between the inside and outside parts :

$$F_{Plfs} = \int_{-\pi/2}^{\pi/2} P \cos\theta \; 2\pi (R_0 + r\cos\theta)\, r\, d\theta$$

$$F_{Plfs} = \pi P r (4R_0 + \pi r)$$

$$F_{Phfs} = -\pi P r (4R_0 - \pi r)$$

The total kinetic pressure force for the whole tore is centrifugal :

$$|F_{Phfs}| < |F_{Plfs}| \qquad F_P = F_{Plfs} + F_{Phfs} = 2\pi^2 r^2 P > 0$$

The kinetic pressure tends to expand radially the tore.
This plasma expansion is due to the tore geometrical shape.

The magnetic pressure : toroidal component

The magnetic pressure is oriented towards the plasma :

$$P_B = \frac{B^2}{2\mu_0} = \frac{B_\phi^2}{2\mu_0} + \frac{B_{r\theta}^2}{2\mu_0}$$

The toroidal magnetic pressure force component is different for high field side and low field side :

$$F_{B_\phi \mathrm{lfs}} = \int_{-\pi/2}^{\pi/2} P_{B_\phi} \cos\theta \; 2\pi \left(R_0 + r\cos\theta\right) r \, d\theta$$

$$P_{B_\phi} = \frac{B_\phi^2}{2\mu_0} = \frac{R_0^2}{R^2} \frac{B_{\phi_0}^2}{2\mu_0} = \frac{R_0^2}{R^2} P_{B_{\phi 0}}$$

$$F_{B_\phi \mathrm{lfs}} = -P_{B_{\phi 0}} \int_{-\pi/2}^{\pi/2} \cos\theta \; 2\pi \frac{R_0^2}{R_0 + r\cos\theta} r \, d\theta$$

$$F_{B_\phi \mathrm{hfs}} = P_{B_{\phi 0}} \int_{-\pi/2}^{\pi/2} \cos\theta \; 2\pi \frac{R_0^2}{R_0 - r\cos\theta} r \, d\theta$$

$$\left|F_{B_\phi \mathrm{hfs}}\right| > \left|F_{B_\phi \mathrm{lfs}}\right| \qquad F_{B_\phi \mathrm{hfs}} + F_{B_\phi \mathrm{lfs}} > 0$$

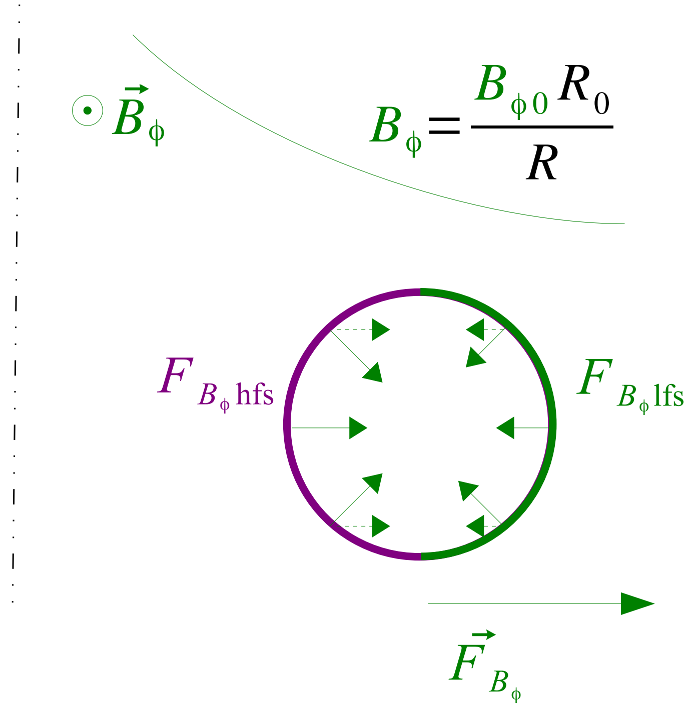

The toroidal magnetic pressure force for the whole tore is centrifugal :
The toroidal magnetic pressure tends to expand radially the plasma.
This plasma expansion is due to the radial toroidal magnetic dependency.

The magnetic pressure : poloidal component

Considering an **uniform toroidal plasma current** $\vec{I}_\phi$ across the plasma poloidal section :
Since the current has a toric shape, the generated poloidal magnetic field component $\vec{B}_{r\theta}$ outside the plasma decreases with the large radius :

$$B_{r\theta} \sim \frac{\mu_0 I_\phi}{2R}$$

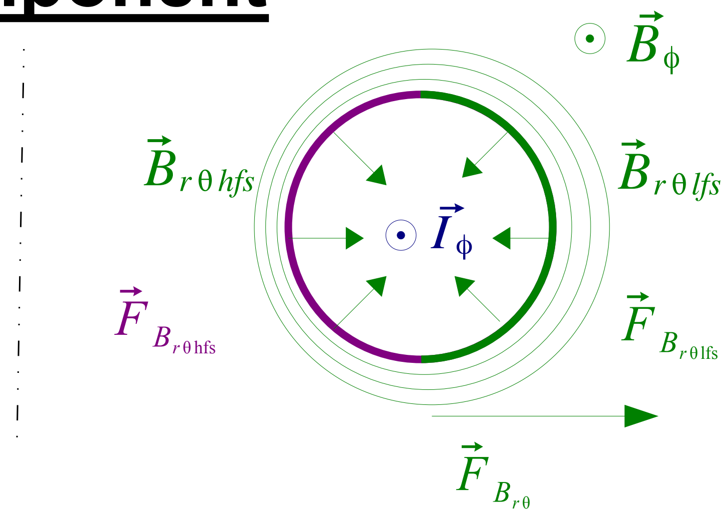

The poloidal magnetic field behaves like the toroidal magnetic component.
The poloidal magnetic pressure force is larger for the inside part of the tore than for the outside part :

$$|F_{B_{r\theta hfs}}| > |F_{B_{r\theta lfs}}| \qquad F_{B_{r\theta hfs}} + F_{B_{r\theta lfs}} > 0$$

The poloidal magnetic pressure force for the whole tore is **centrifugal**.
When the toroidal plasma current is uniform across the plasma, the poloidal magnetic pressure tends to expand radially the plasma.

This effect is changed when the toroidal plasma current is $\vec{I}_\phi$ moved **off-center** or if another poloidal magnetic field component is added.

Active stabilization: additional vertical magnetic component

Plasma can also be stabilized using an additional vertical component.
The effect is obtained through **Laplace force** :

$$\vec{F}_{Bv} = \vec{j} \wedge \vec{B}_v$$

The force due to vertical magnetic component crossing with the toroidal plasma current generate a centripetal force.

The force due to vertical magnetic component crossing with the poloidal plasma current does not change the plasma shape.

This vertical magnetic component can be created by additional horizontal coils, placed in Helmholtz like configuration.

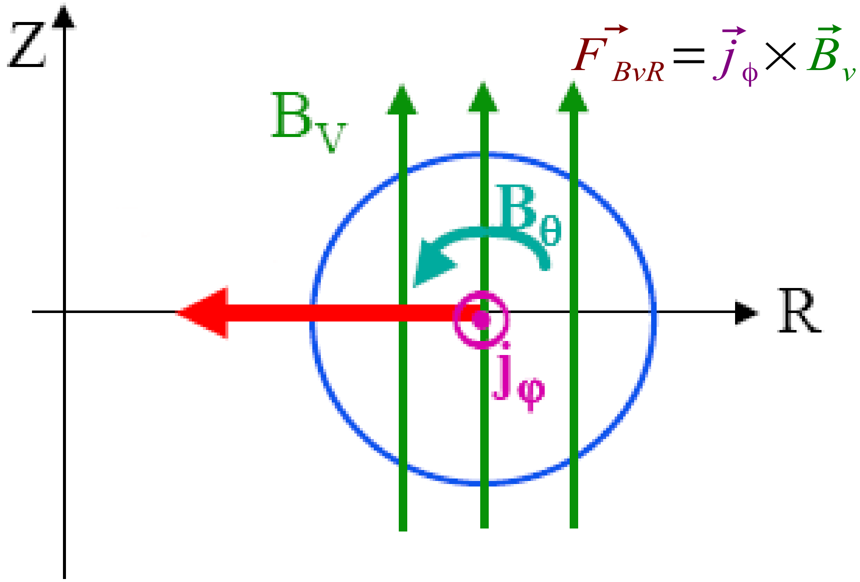

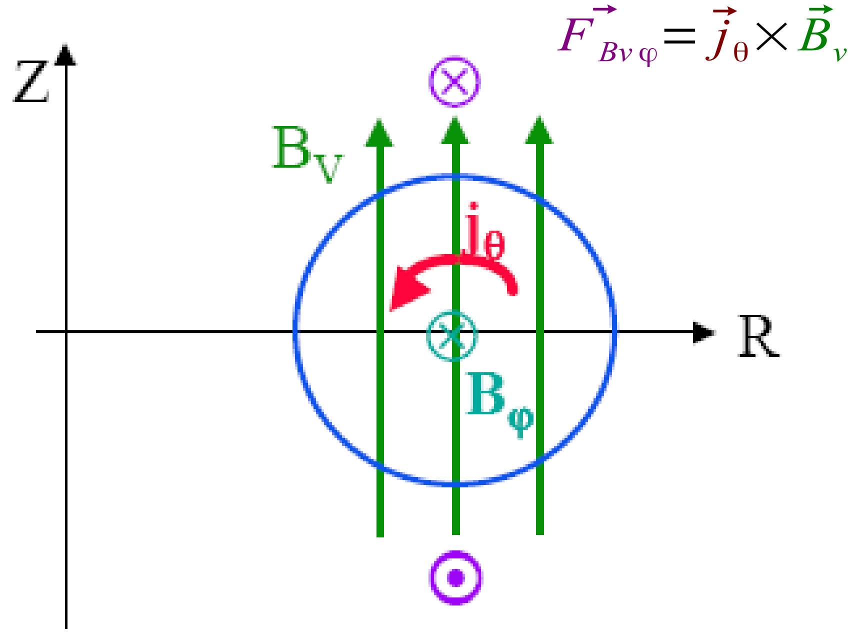

2D axis-symmetric equilibrium : Grad-Shafranov equation

We want to determine the tokamak plasma equilibrium.

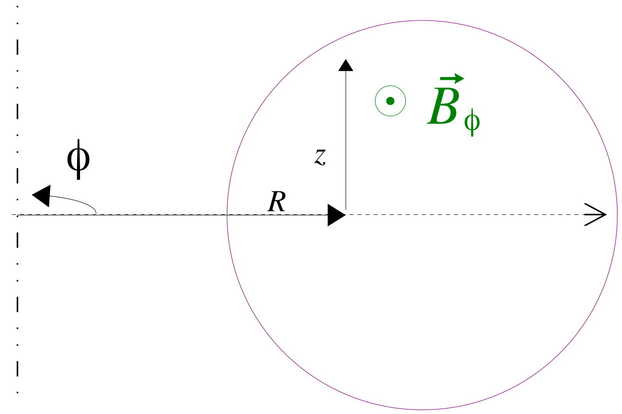

We use the axis-symmetric assumption (independent of ϕ).

- Force balance $\vec{j} \wedge \vec{B} = \vec{\nabla} P$
- Maxwell-Ampere equation $\vec{\nabla} \wedge \vec{B} = \mu_0 \vec{j}$
- Maxwell-Thomson equation $\vec{\nabla} . \vec{B} = 0$

The poloidal magnetic and current fluxes are defined through toroidal disc :

$$\vec{B}_{r\theta} = \vec{B} - \vec{B}_\phi \qquad \vec{j}_{r\theta} = \vec{j} - \vec{j}_\phi$$

$$\psi = \psi_{r\theta} = \frac{1}{2\pi} \iint_{S_R} \vec{B}_{r\theta} . \vec{ds} \qquad I_{r\theta} = \frac{1}{2\pi} \iint_{S_R} \vec{j}_{r\theta} . \vec{ds}$$

$$\psi = R A_\phi \qquad \vec{B}_{r\theta} = \vec{\nabla} \wedge \vec{A}_\phi \qquad I_{r\theta} = \frac{1}{\mu_0} R B_\phi$$

ψ and $I_{r\theta}$ are constant for different discs on the same magnetic flux surfaces.

P and $I_{r\theta}$ are also functions of ψ :

$$P = P(\psi) \qquad I_{r\theta} = I_{r\theta}(\psi)$$

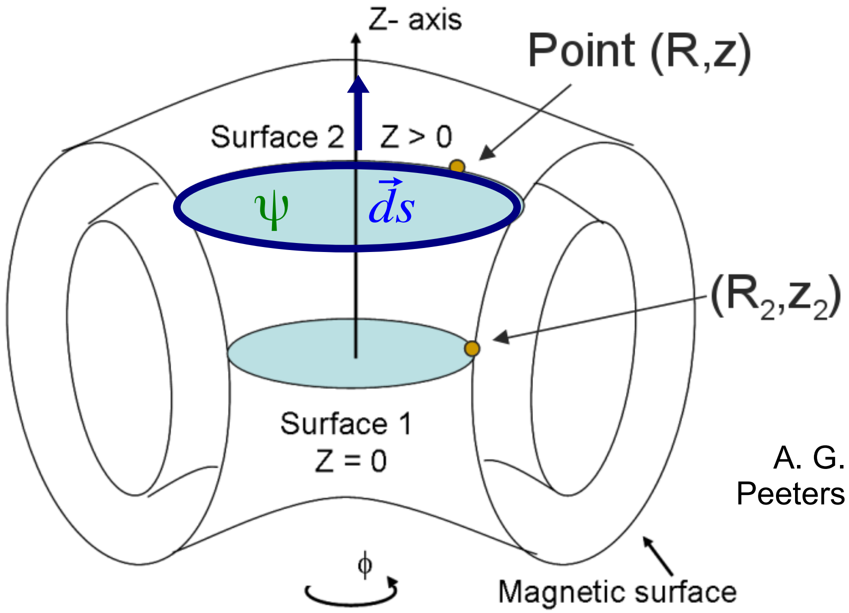

Grad-Shafranov equation

P, $I_{r\theta}$ and ψ variables are linked by Grad-Shafranov equation :

$$\boxed{R\frac{\partial}{\partial R}\frac{1}{R}\frac{\partial\psi}{\partial R}+\frac{\partial^2\psi}{\partial z^2}=-\mu_0 R^2\frac{dP}{d\psi}-\mu_0^2 I_{r\theta}\frac{dI_{r\theta}}{d\psi}}$$

When the pressure and the poloidal current profiles and the edge poloidal magnetic component are known, it is possible to extract the plasma magnetic flux surface shape.

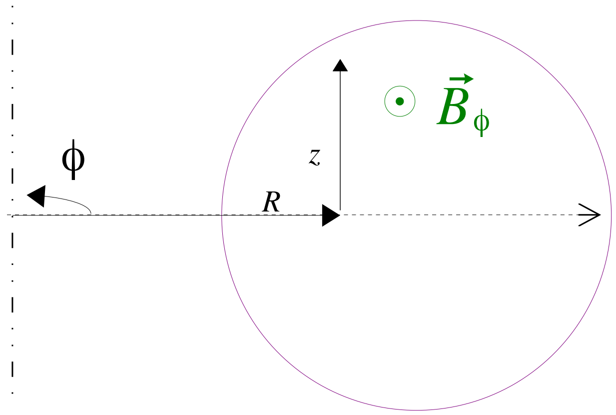

Parameters:

$$\psi=\frac{1}{2\pi}\iint_{S_R}\vec{B}_{r\theta}.\vec{ds}\qquad\qquad \vec{B}_{r\theta}=\vec{\nabla}\wedge\frac{\psi}{R}\vec{e}_\phi$$

$$I_{r\theta}=\frac{1}{2\pi}\iint_{S_R}\vec{j}_{r\theta}.\vec{ds}$$

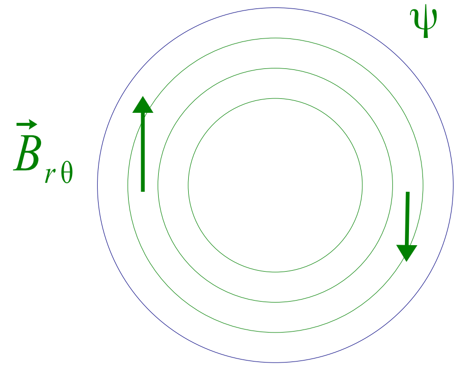

Modified Laplacian operator:

$$\Delta^*=R\frac{\partial}{\partial R}\frac{1}{R}\frac{\partial}{\partial R}+\frac{\partial^2}{\partial z^2}$$

Large aspect ratio

Grad-Shafranov equation:

$$R\frac{\partial}{\partial R}\frac{1}{R}\frac{\partial\psi}{\partial R}+\frac{\partial^2\psi}{\partial z^2}=-\mu_0 R^2\frac{dP}{d\psi}-\mu_0^2 I_{r\theta}\frac{dI_{r\theta}}{d\psi}$$

Solution for a large aspect ratio tore :

$\epsilon=a/R_0\ll 1$ $\qquad R_0$: *last closed flux surface large radius*

Tore coordinate system (r,θ)

$$R=R_0+r\cos\theta$$
$$z=r\sin\theta$$

ψ perturbative development : $\psi(r,\theta)=\psi_0(r)+\psi_1(r,\theta)$

$\psi_0(r)$: (non perturbed) concentric cylindrical solution

$$\psi_0(R,z)=\psi_0(R_0+r\cos\theta,r\sin\theta)$$

$$\frac{\partial\psi_0}{\partial\theta}=0 \qquad \vec{\nabla}\psi_0=\frac{d\psi_0}{dr}\vec{e}_r \qquad \vec{e}_r=\cos\theta\,\vec{e}_R+\sin\theta\,\vec{e}_z$$

$$\frac{\partial\psi_0}{\partial R}=\cos\theta\frac{d\psi_0}{dr} \qquad \frac{\partial\psi_0}{\partial z}=\sin\theta\frac{d\psi_0}{dr}$$

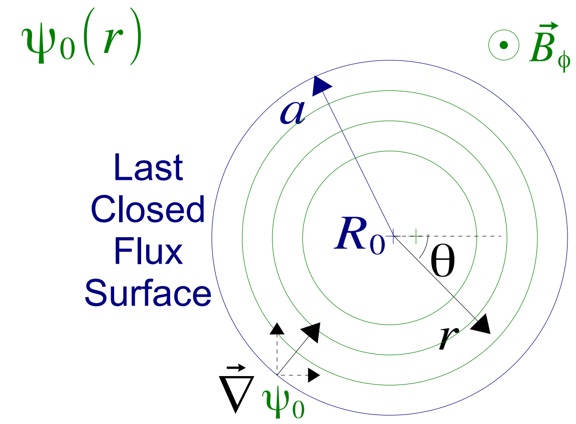

$\psi_1(r,\theta)$: toroidal perturbation

$\Delta(r)$: inner magnetic surface decentering (Shafranov shift)

$$\psi(R,z)=\psi_0(R_0-\Delta(r)+r\cos\theta,r\sin\theta) \qquad \Delta(a)=0$$

$$\psi(R,z)=\psi_0(R,z)-\Delta(r)\cos\theta\frac{d\psi_0}{dr}$$

$$\psi_1(R,z)=-\Delta(r)\cos\theta\frac{d\psi_0}{dr}=-\Delta(r)\frac{\partial\psi_0}{\partial R}$$

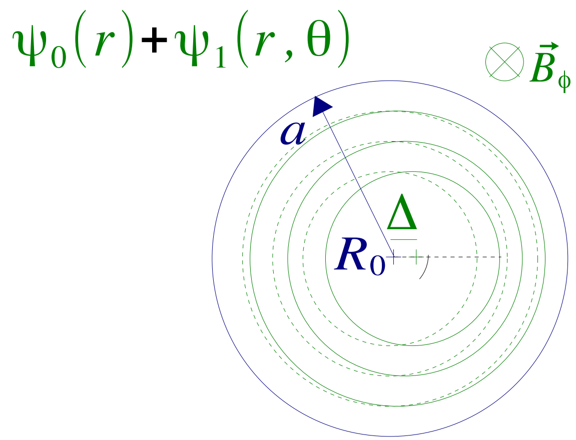

Shafranov perturbative development

$$R=R_0+r\cos\theta \qquad z=r\sin\theta$$

$$\frac{\partial\psi_0}{\partial R}=\cos\theta\frac{\partial\psi_0}{\partial r} \qquad \frac{\partial\psi_0}{\partial z}=\sin\theta\frac{\partial\psi_0}{\partial r}$$

$$\frac{\partial\psi_0}{\partial\theta}=0$$

Grad-Shafranov equation in (r,θ) coordinate system :

$$R\frac{\partial}{\partial R}\frac{1}{R}\frac{\partial\psi}{\partial R}+\frac{\partial^2\psi}{\partial z^2}=-\mu_0R^2\frac{dP}{d\psi}-\mu_0^2I_{r\theta}\frac{dI_{r\theta}}{d\psi}$$

$$\frac{1}{r}\frac{\partial}{\partial r}r\frac{\partial\psi}{\partial r}+\frac{1}{r^2}\frac{\partial^2\psi}{\partial\theta^2}-\frac{1}{R_0+r\cos\theta}\left(\cos\theta\frac{\partial\psi}{\partial r}-\frac{\sin\theta}{r}\frac{\partial\psi}{\partial\theta}\right)=-\mu_0(R_0+r\cos\theta)^2\frac{dP}{d\psi}-\mu_0^2I_{r\theta}\frac{dI_{r\theta}}{d\psi}$$

cylindrical part *toroidal correction*

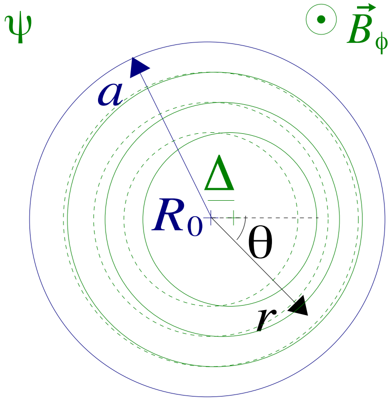

Cylindrical equation (leading order):

$$\frac{1}{r}\frac{\partial}{\partial r}r\frac{\partial\psi_0}{\partial r}+\frac{1}{r^2}\frac{\partial^2\psi_0}{\partial\theta^2}=-\mu_0R_0^2\frac{dP}{d\psi_0}-\mu_0^2I_{r\theta}\frac{dI_{r\theta}}{d\psi_0}$$

Toroidal correction (1st order):

$$\frac{1}{r}\frac{\partial}{\partial r}r\frac{\partial\psi_1}{\partial r}+\frac{1}{r^2}\frac{\partial^2\psi_1}{\partial\theta^2}-\frac{\cos\theta}{R_0}\frac{\partial\psi_0}{\partial r}=-\frac{d}{dr}\left(-\mu_0R_0^2\frac{dP}{d\psi_0}+\mu_0^2I_{r\theta}\frac{dI_{r\theta}}{d\psi_0}\right)\frac{dr}{d\psi_0}\psi_1-2\mu_0R_0r\cos\theta\frac{dP}{d\psi_0}$$

ψ_1 is replaced with Δ:

$$\psi_1(R,z)=-\Delta(r)\cos\theta\frac{d\psi_0}{dr}$$

$$-\Delta\frac{d}{dr}\left(\frac{1}{r}\frac{\partial}{\partial r}r\frac{\partial\psi_0}{\partial r}\right)+\frac{1}{r}\frac{dr}{d\psi_0}\frac{d}{dr}\left[r\left(\frac{d\psi_0}{dr}\right)^2\frac{d\Delta}{dr}\right]-\frac{1}{R_0}\frac{\partial\psi_0}{\partial r}=\Delta\frac{d}{dr}\left(\mu_0R_0^2\frac{dP}{d\psi_0}+\mu_0^2I_{r\theta}\frac{dI_{r\theta}}{d\psi_0}\right)-2\mu_0R_0r\frac{dP}{dr}\frac{dr}{d\psi_0}$$

Using the cylindrical equation:

$$\frac{1}{r}\frac{dr}{d\psi_0}\frac{d}{dr}\left[r\left(\frac{d\psi_0}{dr}\right)^2\frac{d\Delta}{dr}\right]-\frac{1}{R_0}\frac{\partial\psi_0}{\partial r}=-2\mu_0R_0r\frac{dP}{dr}\frac{dr}{d\psi_0}$$

Equilibrium Shafranov shift

$\psi = R A_\phi \qquad \left(\vec{B} = \vec{\nabla} \wedge \vec{A}\right)$

$\vec{B}_r + \vec{B}_\theta = \vec{\nabla} \wedge \frac{\psi}{R} \vec{e}_\phi$

Flux decentering $\Delta(r)$ equation:

$$\frac{1}{r}\frac{dr}{d\psi_0}\frac{d}{dr}\left[r\left(\frac{d\psi_0}{dr}\right)^2\frac{d\Delta}{dr}\right] - \frac{1}{R_0}\frac{\partial\psi_0}{\partial r} = -2\mu_0 R_0 r \frac{dP}{dr}\frac{dr}{d\psi_0}$$

The poloidal magnetic field is deduced from the flux:

$$B_{\theta 0} = \frac{1}{R}\frac{d\psi_0}{dr}$$

The decentering Δ is function of P and $B_{\theta 0}$

$$\frac{d}{dr}\left(r R_0 B_{\theta 0}^2 \frac{d\Delta}{dr}\right) = 2\mu_0 r^2 \frac{dP}{dr} - B_{\theta 0}^2 r$$

$$r R_0 B_{\theta 0}^2 \frac{d\Delta}{dr} = 2\mu_0 r^2 P - 4\mu_0 \int_0^r \hat{r} P \, d\hat{r} - \int_0^r \hat{r} B_{\theta 0}^2 \, d\hat{r}$$

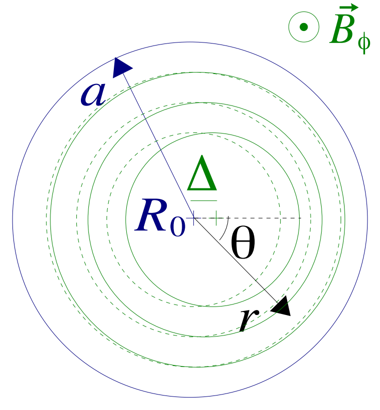

2 main dimensionless variables appear for the edge (a):

$$\beta_p = \frac{4\mu_0}{a^2 B_{\theta 0}^2(a)} \int_0^a r P \, dr$$

$$l_i = \frac{2}{a^2 B_{\theta 0}^2(a)} \int_0^a r B_{\theta 0}^2 \, dr \qquad l_i \sim \ln\left(1.65 + 0.89 \frac{q_a - q_0}{q_0}\right) \qquad \text{internal inductance}: L_i = \frac{1}{2}\mu_0 R_0 l_i$$

Decentering properties:

$$\Delta(a) = 0 \qquad \frac{d\Delta}{dr}(a) = -\frac{a}{R_0}\left(\beta_p + \frac{1}{2} l_i\right) \qquad \left(P(a) = 0\right)$$

$$\frac{d\Delta}{dr}(0) = 0$$

Approximated decentering shape: $\Delta(r) \sim \frac{a^2 - r^2}{2R_0}\left(\beta_p + \frac{1}{2} l_i\right)$ $\qquad \Delta(0) \sim \frac{a^2}{2R_0}\left(\beta_p + \frac{1}{2} l_i\right)$

Poloidal magnetic field at the plasma edge

$$\psi(R,z)=\psi_0(R,z)-\Delta(r)\cos\theta\frac{d\psi_0}{dr}$$

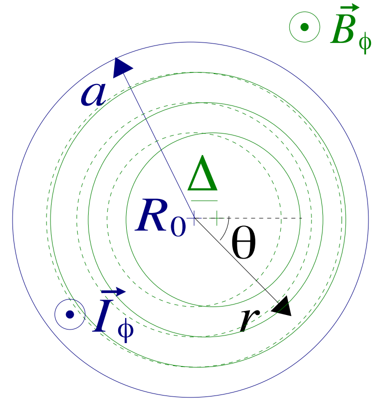

Poloidal magnetic field B_θ :

$$B_{r\theta}=\frac{1}{R_0+r\cos\theta}\frac{d\psi}{dr} \qquad \vec{B}_{r\theta}=\vec{\nabla}\wedge\frac{\psi}{R}\vec{e}_\phi$$

Poloidal magnetic field at the edge:

$$B_\theta(a)=B_{\theta 0}(a)\left[1-\left(\frac{a}{R_0}+\frac{d\Delta}{dr}(a)\right)\cos\theta\right] \qquad B_r(a)=0$$

Since:

$$\frac{d\Delta}{dr}(a)=-\frac{a}{R_0}\left(\beta_p+\frac{1}{2}L_i\right)$$

$$\boxed{B_\theta(a)=B_{\theta 0}(a)\left(1+\frac{a}{R_0}\Lambda\cos\theta\right)} \qquad \Lambda=\beta_p+\frac{1}{2}l_i-1$$

The poloidal magnetic field is larger on the low field side.
It is linked to the flux surface decentering.

Poloidal magnetic field cylindrical approximation is directly linked to the plasma toroidal current

$$B_{\theta 0}(a)=\frac{\mu_0 I_\phi}{2\pi a} \qquad I_P=I_\phi$$

External solution connected to the equilibrium

Outside the plasma $r \geq a$ Grad-Shafranov equation in vacuum:

$$R\frac{\partial}{\partial R}\frac{1}{R}\frac{\partial \psi}{\partial R}+\frac{\partial^2 \psi}{\partial z^2}=0$$

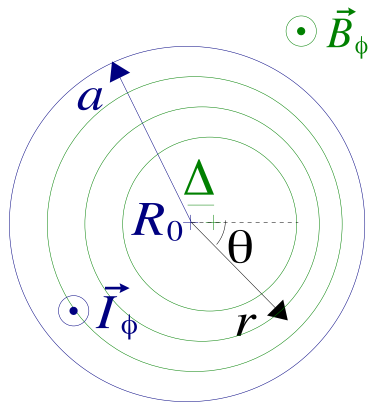

For large aspect ratio:

$$\frac{1}{r}\frac{\partial}{\partial r}r\frac{\partial \psi}{\partial r}+\frac{1}{r^2}\frac{\partial^2 \psi}{\partial \theta^2}-\frac{1}{R_0+r\cos\theta}\left(\cos\theta\frac{\partial \psi}{\partial r}-\frac{\sin\theta}{r}\frac{\partial \psi}{\partial \theta}\right)=0$$

Solutions with the **internal plasma current** I_ϕ :

$$\psi(r,\theta)=-\frac{\mu_0 R_0 I_\phi}{2\pi}\left(\ln\frac{8R_0}{r}-2\right)-\frac{\mu_0 I_\phi}{4\pi}\left[r\left(\ln\frac{8R_0}{r}-1\right)+c_1\frac{a^2}{r}+c_2 r\right]\cos\theta$$

$$B_\theta(r,\theta)=\frac{\mu_0 I_\phi}{2\pi r}+\frac{\mu_0 I_\phi}{2\pi R_0}\frac{1}{2}\left(-\ln\frac{8R_0}{r}+c_1\frac{a^2}{r^2}-c_2\right)\cos\theta$$

$$B_\theta=\frac{1}{R}\frac{\partial \psi}{\partial r}$$

$$B_r(r,\theta)=\frac{\mu_0 I_\phi}{2\pi R_0}\frac{1}{2}\left(-\ln\frac{8R_0}{r}+1-c_1\frac{a^2}{r^2}-c_2\right)\sin\theta$$

$$B_r=-\frac{1}{Rr}\frac{\partial \psi}{\partial \theta}$$

Connection with the internal equilibrium :

$$B_\theta(a,\theta)=B_{\theta 0}(a)\left(1+\frac{a}{R_0}\Lambda\cos\theta\right) \Rightarrow c_1-c_2=\ln\frac{8R_0}{a}+2\Lambda$$

$$B_r(a,\theta)=0 \Rightarrow c_1+c_2=-\ln\frac{8R_0}{a}+1$$

$$\Rightarrow \quad c_1=\Lambda+\frac{1}{2} \qquad c_2=-\left(\ln\frac{8R_0}{a}+\Lambda-\frac{1}{2}\right)$$

External solution connected to the equilibrium:

$$\psi(r,\theta)=-\frac{\mu_0 R_0 I_\phi}{2\pi}\left(\ln\frac{8R_0}{r}-2\right)+\frac{\mu_0 I_\phi}{4\pi}\left(1-\frac{a^2}{r^2}\right)\left(\Lambda+\frac{1}{2}\right)r\cos\theta$$

External flux with no external poloidal magnetic field

ψ equilibrium solution with internal plasma current :

$$\psi(r,\theta)=-\frac{\mu_0 R_0 I_\phi}{2\pi}\left(\ln\frac{8R_0}{r}-2\right)-\frac{\mu_0 I_\phi}{4\pi}\left[r\left(\ln\frac{8R_0}{r}-1\right)+c_1\frac{a^2}{r}+c_2 r\right]\cos\theta$$

$$B_r(r,\theta)=\frac{\mu_0 I_\phi}{2\pi R_0}\frac{1}{2}\left(-\ln\frac{8R_0}{r}+1-c_1\frac{a^2}{r^2}-c_2\right)\sin\theta$$

ψ_i solution with internal plasma current, and **with no external poloidal field**

Conditions :

$$\psi_i(+\infty,\theta)=0 \quad\Rightarrow\quad c_{i2}=0$$

$$B_{ir}(a,\theta)=0 \quad\Rightarrow\quad c_{i1}=-\ln\frac{8R_0}{a}+1$$

$$\psi_i(r,\theta)=-\frac{\mu_0 R_0 I_\phi}{2\pi}\left(\ln\frac{8R_0}{r}-2\right)-\frac{\mu_0 I_\phi}{4\pi}\left(1-\frac{a^2}{r^2}\right)\left(\ln\frac{8R_0}{r}-1\right)r\cos\theta$$

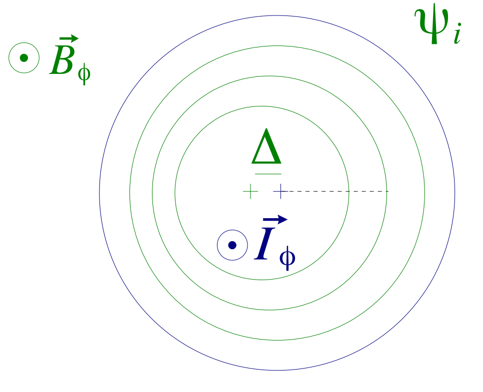

Magnetic flux surfaces are decentered inwards:

$$B_{i\theta}(a,\theta)=B_{i\theta 0}(a)\left[1-\frac{a}{R_0}\left(\ln\frac{8R_0}{a}-\frac{1}{2}\right)\cos\theta\right]$$

External flux with no external poloidal magnetic field

In order to get the equilibrium solution,

$$\psi(r,\theta)=-\frac{\mu_0 R_0 I_\phi}{2\pi}\left(\ln\frac{8R_0}{r}-2\right)+\frac{\mu_0 I_\phi}{4\pi}\left(1-\frac{a^2}{r^2}\right)\left(\Lambda+\frac{1}{2}\right)r\cos\theta$$

because the solution with no external magnetic field is different,

$$\psi_i(r,\theta)=-\frac{\mu_0 R_0 I_\phi}{2\pi}\left(\ln\frac{8R_0}{r}-2\right)-\frac{\mu_0 I_\phi}{4\pi}\left(1-\frac{a^2}{r^2}\right)\left(\ln\frac{8R_0}{r}-1\right)r\cos\theta$$

an external magnetic flux must be added : ψ_e

$$\psi_e(r,\theta)=\psi(r,\theta)-\psi_i(r,\theta)=\frac{\mu_0 I_\phi}{4\pi}\left(1-\frac{a^2}{r^2}\right)\left(\ln\frac{8R_0}{r}+\Lambda-\frac{1}{2}\right)(R-R_0)$$

This flux mainly corresponds a vertical magnetic field component :

$$\vec{B}_e=\vec{\nabla}\wedge\frac{\psi_e}{R}\vec{e}_\phi\sim\frac{\mu_0 I_\phi}{4\pi R_0}\left(1-\frac{a^2}{r^2}\right)\left(\ln\frac{8R_0}{r}+\Lambda-\frac{1}{2}\right)\vec{e}_z$$

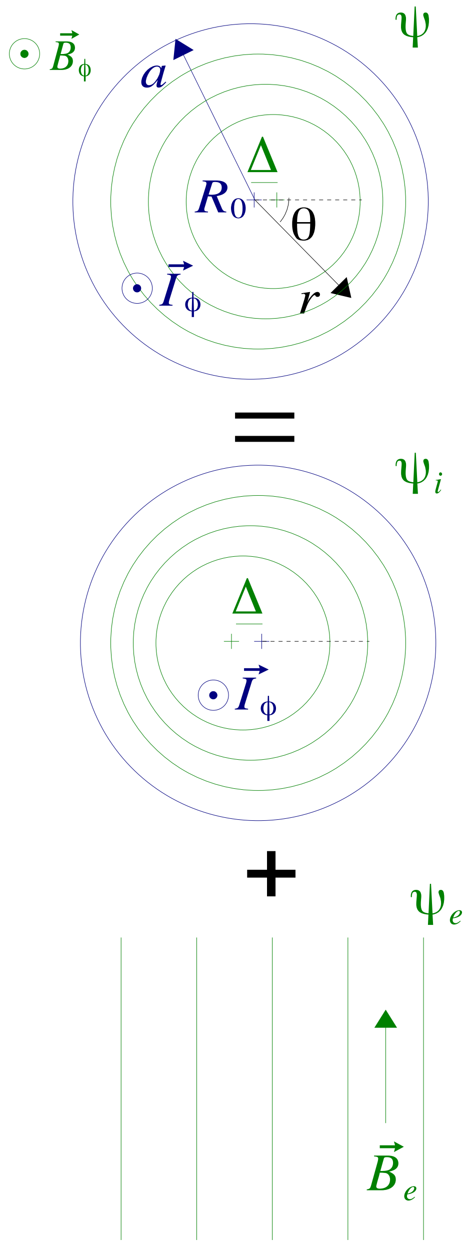

Passive stabilization : the conductive wall

The kinetic and magnetic pressures tend to expand the plasma radially.

If the plasma is surrounded with a **conductive wall** :
The poloidal magnetic field can not penetrate the metallic wall.
When the plasma tends to expand radially, the poloidal magnetic field lines are crushed together between the plasma and the wall : the poloidal magnetic increases on the outside part $\vec{B}_{\theta lfs}$ and decreases on the inside part of the tore $\vec{B}_{\theta hfs}$.
The **poloidal magnetic pressure** force change direction : it becomes **centripetal**.

This method does not work for time longer than typical **wall electrical resistance time** : above the resistive time, the wall response is different.

This method was used on first tokamaks to get short time MHD stability.

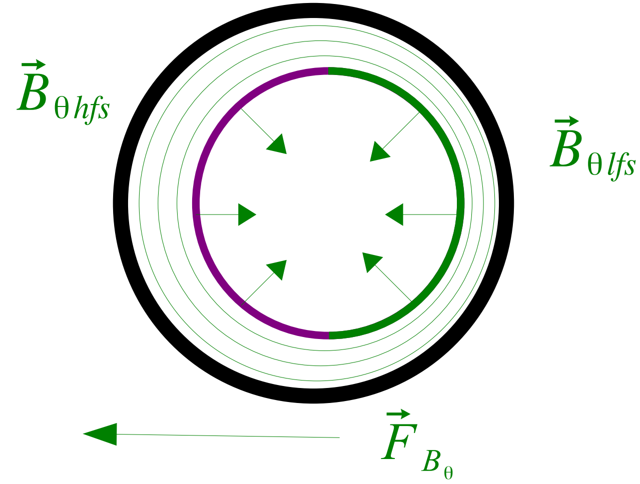

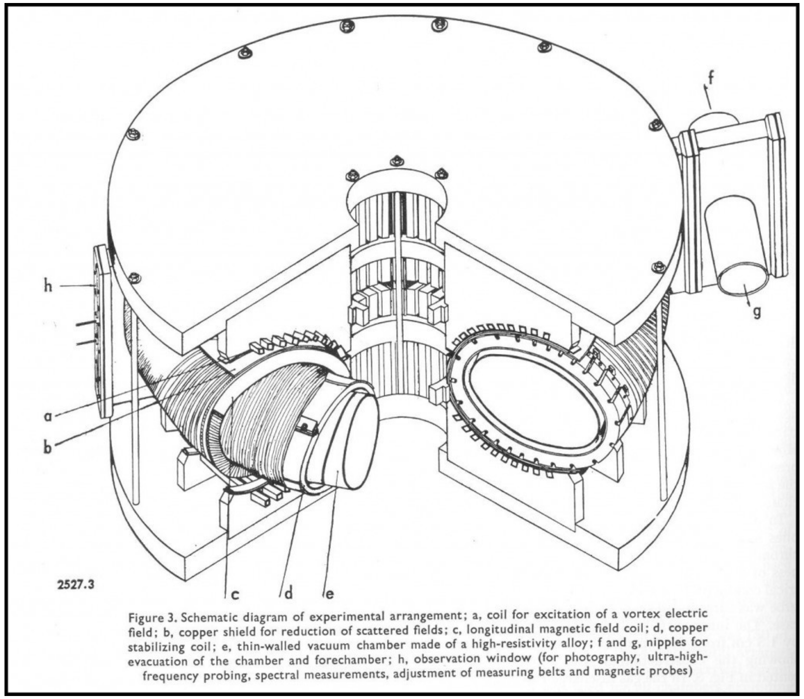

Figure 3. Schematic diagram of experimental arrangement; a, coil for excitation of a vortex electric field; b, copper shield for reduction of scattered fields; c, longitudinal magnetic field coil; d, copper stabilizing coil; e, thin-walled vacuum chamber made of a high-resistivity alloy; f and g, nipples for evacuation of the chamber and forechamber; h, observation window (for photography, ultra-high-frequency probing, spectral measurements, adjustment of measuring belts and magnetic probes)

Tokamak T1 : (e) thin-walled vacuum chamber made of high resistive alloy

Conductive wall and magnetic fields

Usual material :
The magnetic field can penetrate the material

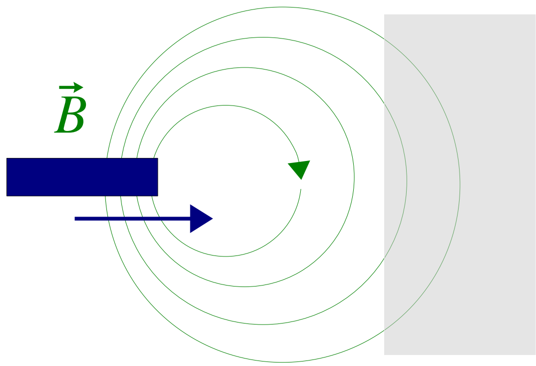

Supra-conductor
= perfect diamagnetism:
eddy currents are driven by the induced voltages created by a changing magnetic field. It prevents magnetic flux from entering a perfect conductor

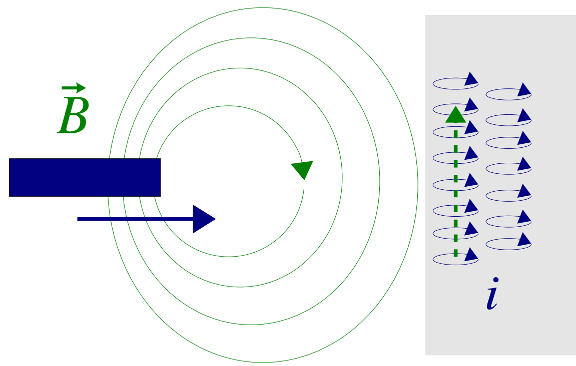

Conductor with finite resistivity :
Ordinary metals are good enough conductors to do this temporarily, until the currents generating the counter-field are dissipated by resistance

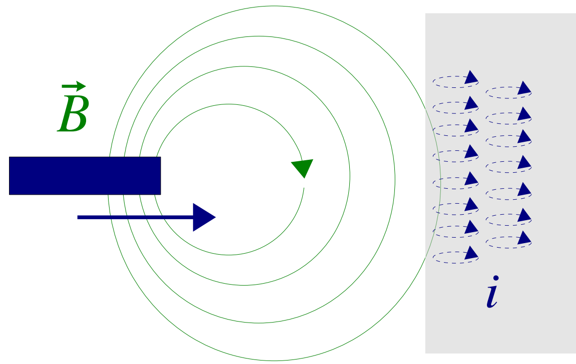

Active Control shaping using toroidal coils

The current in **external toroidal coils** attracts the magnetic surfaces, if this current is the same direction as the plasma toroidal current. This current repulses the magnetic surfaces if they both currents are in opposite directions.

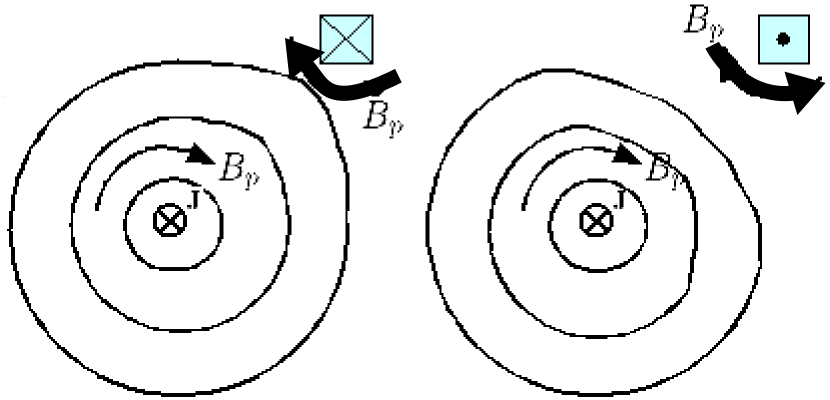

Arthur G. Peeters, Warwick Univ.

Plasma position control

This property allows to control the plasma position across the chamber, in order to avoid the plasma to reach the wall.

Plasma shaping

This property allows to give the plasma the shape corresponding to the best MHD stability and the best confinement.

Plasma elongation

Plasma vertical elongation allows to create the X point divertor above or beneath the plasma.
For the same q profile, the toroidal plasma current can be larger.

Circular plasma : $q_a = \frac{a B_\phi}{R B_\theta} = \frac{2\pi a^2 B_\phi}{\mu_0 R I_p}$ $\qquad B_\theta(r) = \frac{\mu_0}{2\pi r} I_p(r)$

Elongated plasma : $q = \frac{2\pi a b B_\phi}{\mu_0 R I_p}$

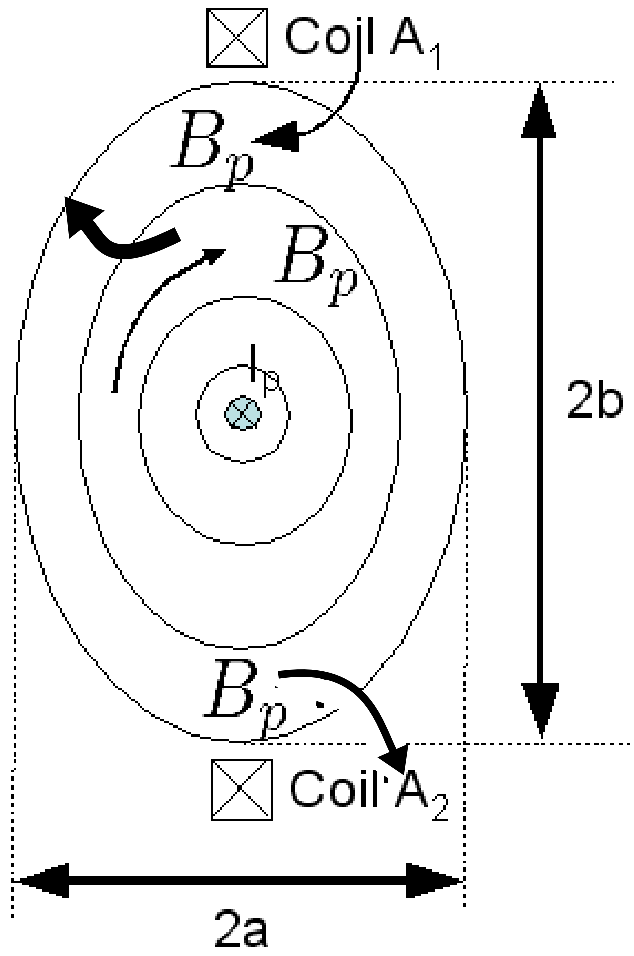

If the current inside coils above and beneath the plasma are identical, the plasma is balanced vertically.

Plasma elongation : $\kappa_a = b/a$

Plasma shaping : circular shaping with limiter

In the simplest plasma shaping, equilibrium magnetic flux surfaces are fitted together. Tores are **not concentric** to balance the centrifugal force due to kinetic and magnetic toroidal pressure asymmetry
The former Tore Supra Tokamak had this configuration.

For this configuration, a magnetic flux surface plays a particular role : this is the first that touches tangentially the internal chamber wall, the **Last Closed Flux Surface**. The contact wall is the **limiter**. It depends on the plasma position inside the chamber.

All magnetic flux surfaces inside the LCFS do not touch the wall : this the **plasma core**.

All magnetic flux surfaces outside the LCFS touch the wall, this is the **Scrape Off Layer**. Because of the wall contact, the SOL plasma is very different than the the core plasma.

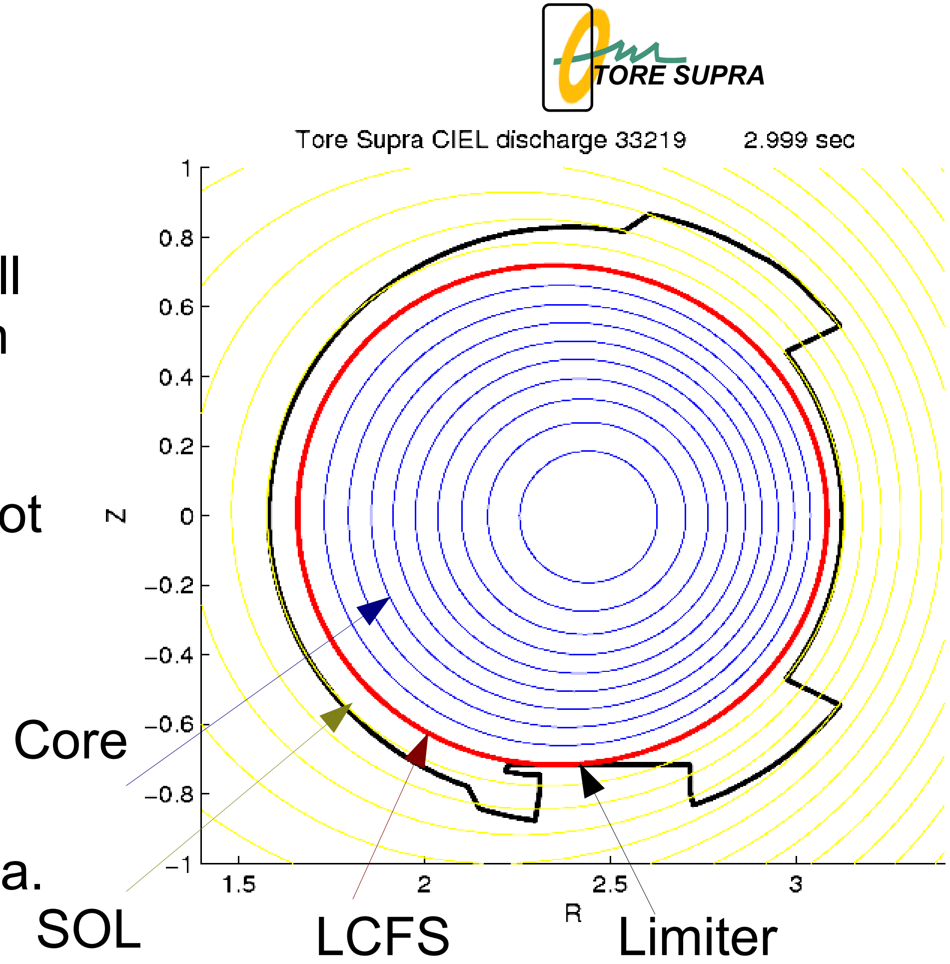

Tore supra plasma

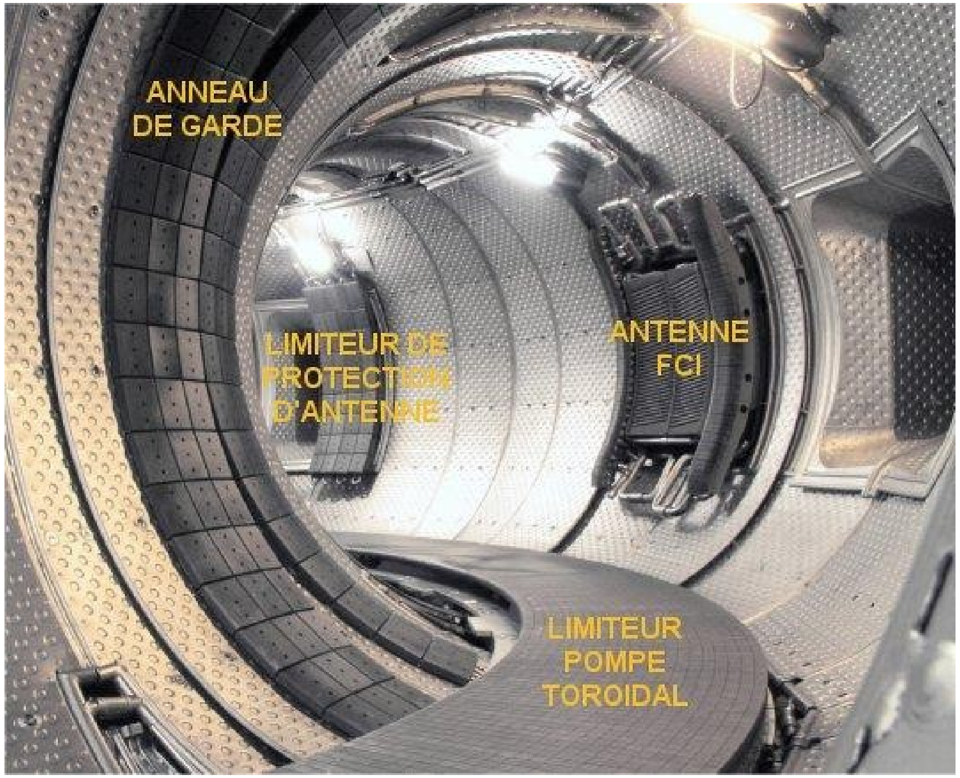

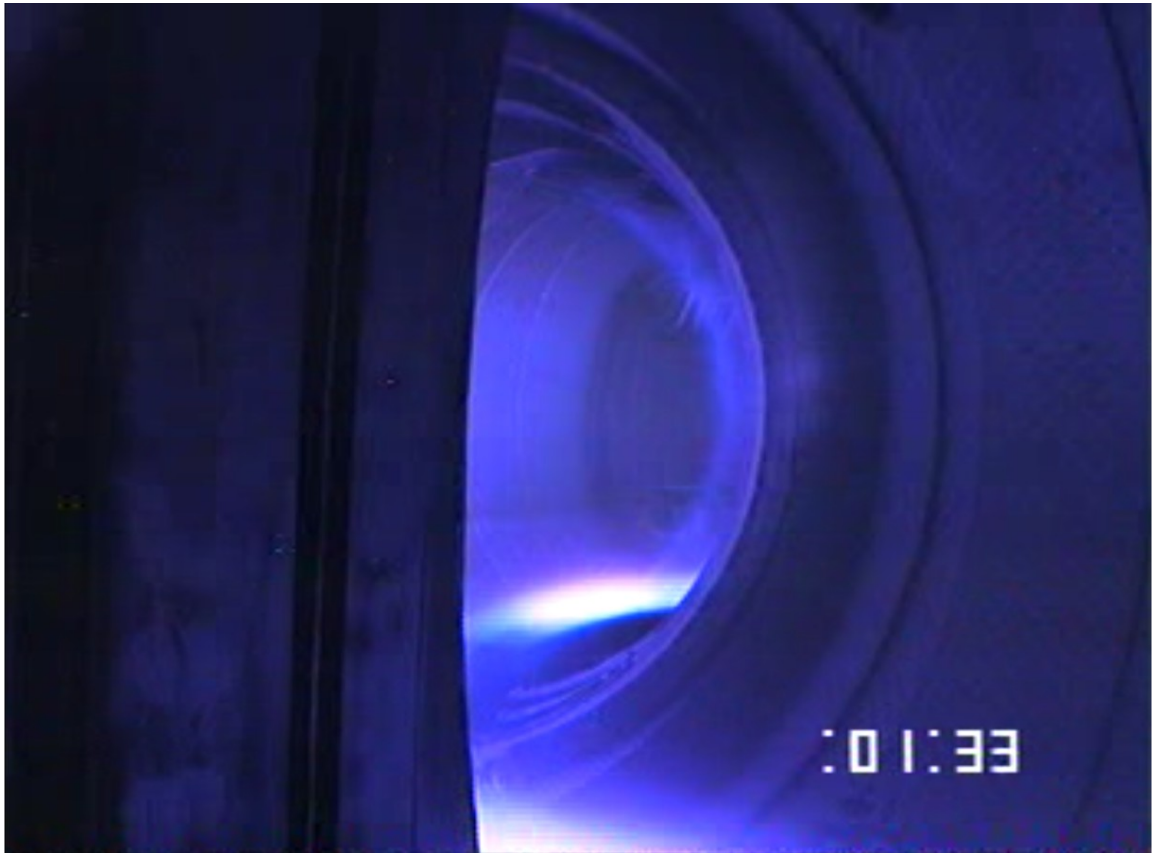

The main limiter used during the main part of the shot plays an important role to extract the plasma power.

X point divertor plasma

In order to improve the **plasma stability**, it is interesting to elongate vertically the plasma. The plasma shaping toroidal coils allow to create a poloidal magnetic field **null point**. This magnetic configuration is a **X point divertor**.
The magnetic flux surface through the null point is **the separatrix**.

The magnetic flux surfaces inside the separatrix are closed : this the plasma core.
This part of the plasma is not in direct contact with the plasma facing components (the targets). The neutral particles extracted from the wall do not reach directly the plasma core. **The core plasma is well protected from the wall**.

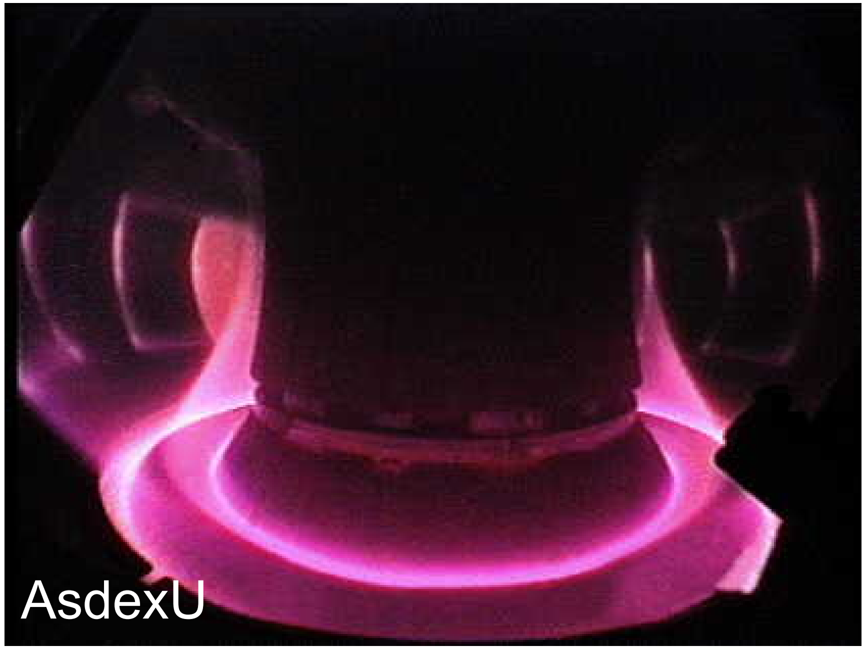

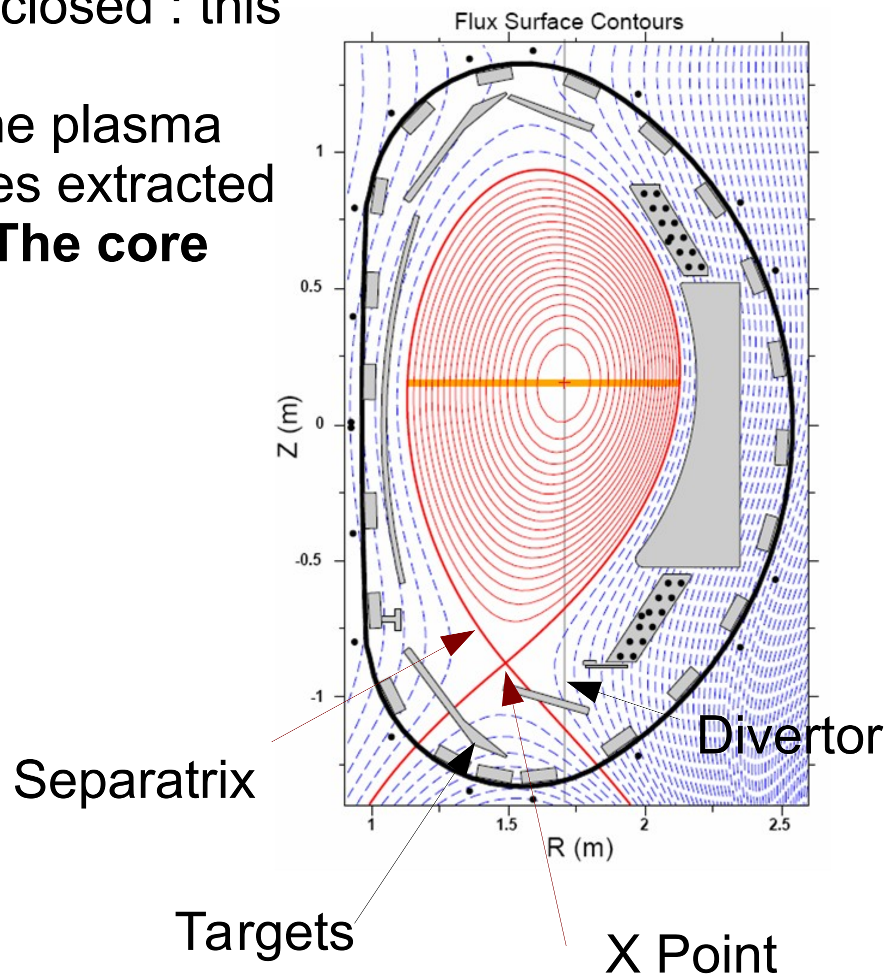

Plasma equilibrium and shaping : ITER

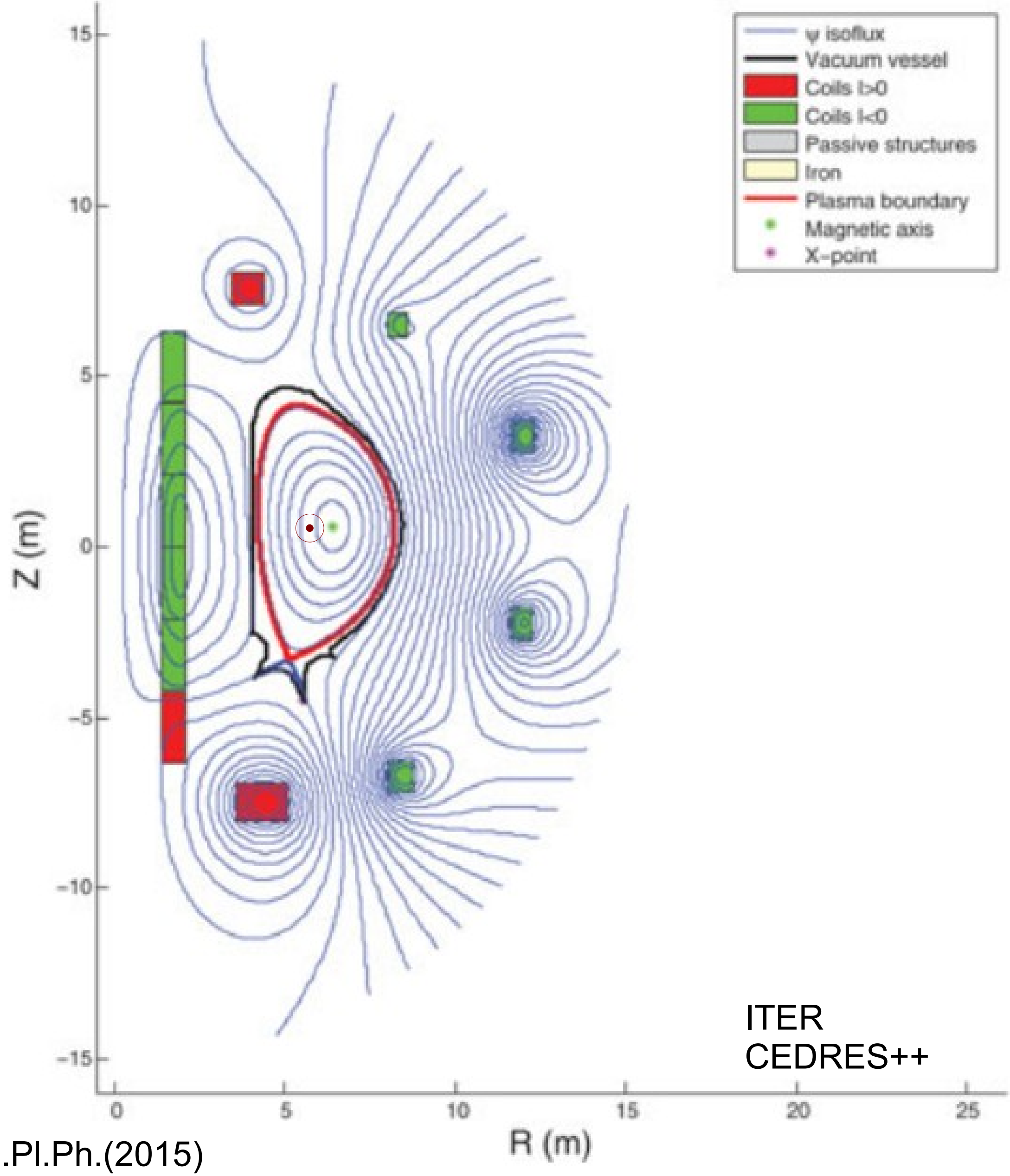

H. Heumann, J.Pl.Ph.(2015)

Plasma shot scenario

Ohmic current generation

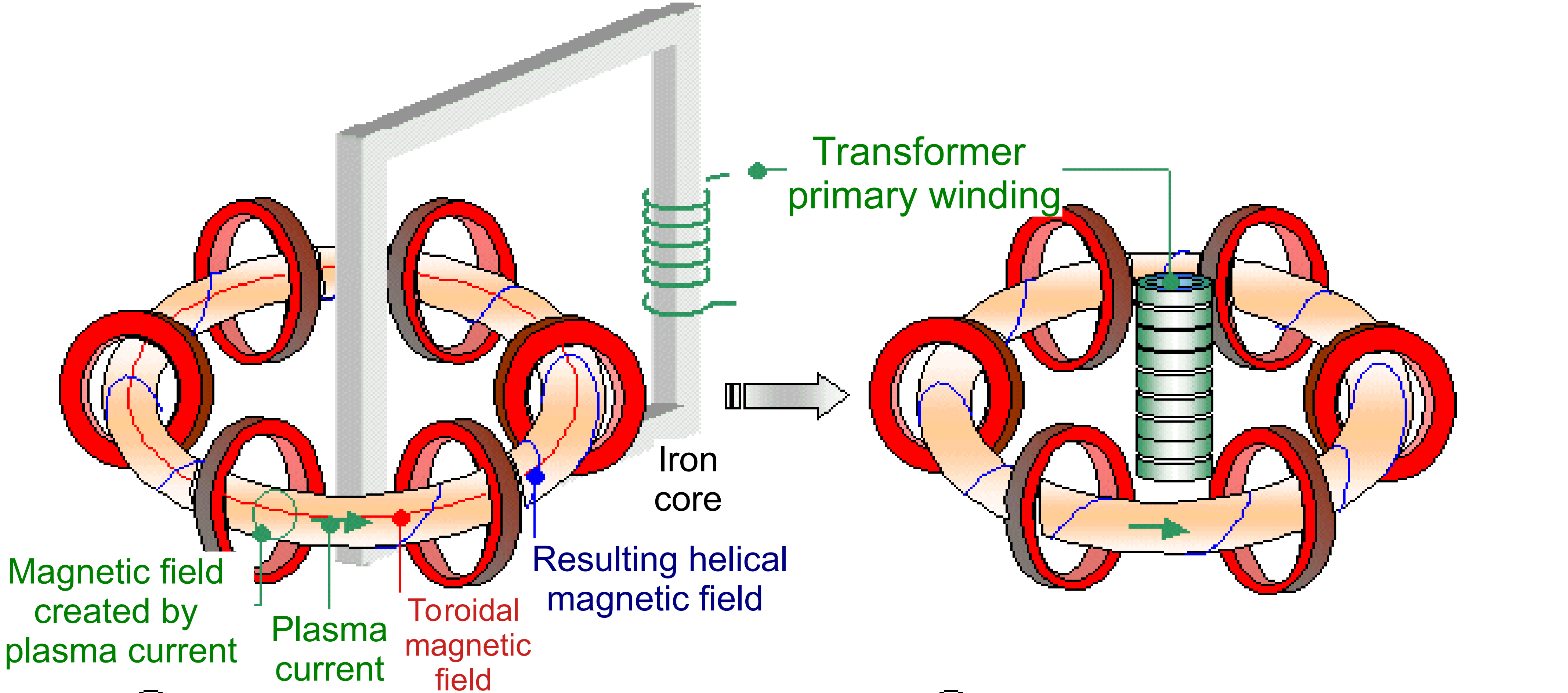

⑦ Tokamak with iron core

⑧ Tokamak without iron core

Plasma generation

- Poloidal Field = induction and equilibrium of plasma current
- PF system on TORE SUPRA: 9 copper coils, associated with 9 power supplies
  - G0 power supply (nominal: *current ± 40 kA*, *voltage ± 1.4 kV*) in parallel with:
    - * the A coil (central solenoid)
    - * 8 circuits (*Bh, Bb, Dh, Db, Eh, Eb, Fh, Fb* coils, each of them in serie with its power supply, respectively *G1h, G1b, G2h, G2b, G3h, G3b, G4h, G4b*)
  - magnetic circuit (cylindrical central post, 6 return arms with rect. cross section ≅ 1 m²)
  - total installed power: *≅ 240 MW*

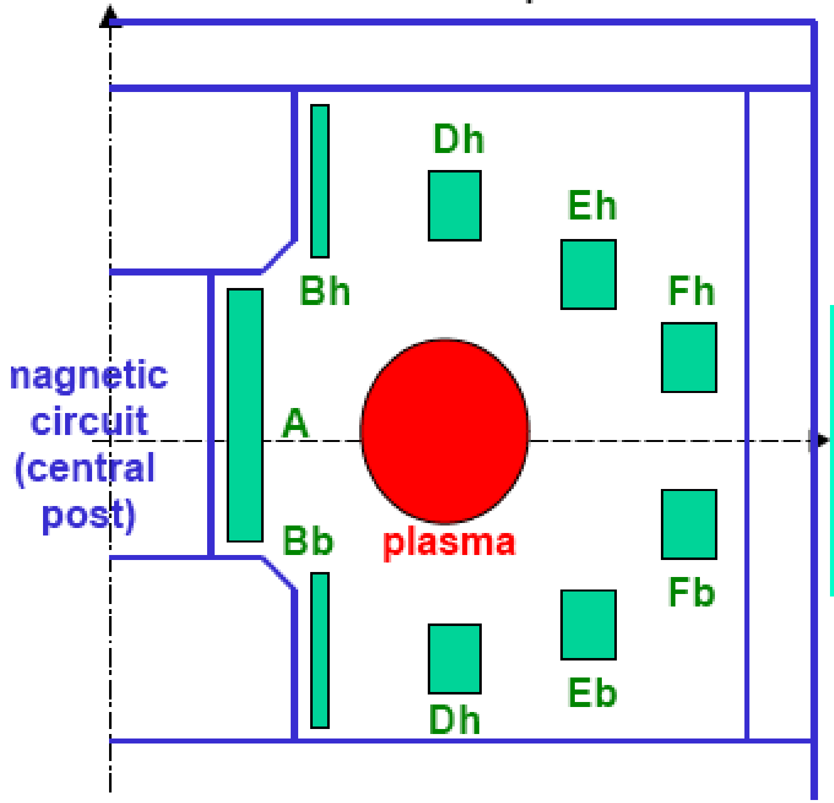

Maximum currents (due to power supply limits)

(>> thermal limit of coils in continuous operating)

A coil (195 turns)	I_{max} = -40 kA/+40 kA
B coils (176 turns)	I_{max} = -5.3 kA/+6.8 kA
D coils (95 turns)	I_{max} = -2.8 kA/+2.7 kA
E coils (96 turns)	I_{max} = -4.4 kA/+1.6 kA
F coils (96 turns)	I_{max} = -4.4 kA/+1.6 kA

Flux consumption

- **Flux consumption: limitation of plasma flat top duration**
  - due to limit on I_{G0} (end of pre-magnetisation and end of flat top)
  - with enough LHCD (3 MW) and I_p < 600 kA: ≅ no theoretical limit

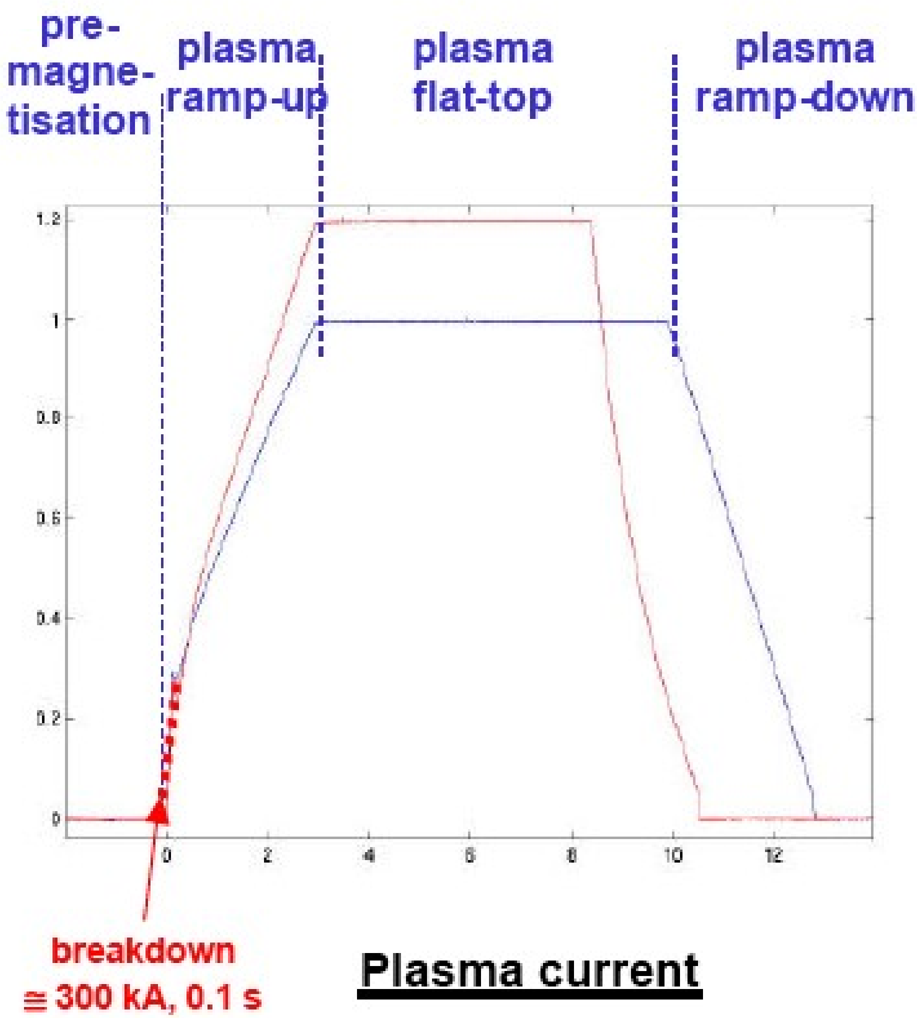

Plasma current

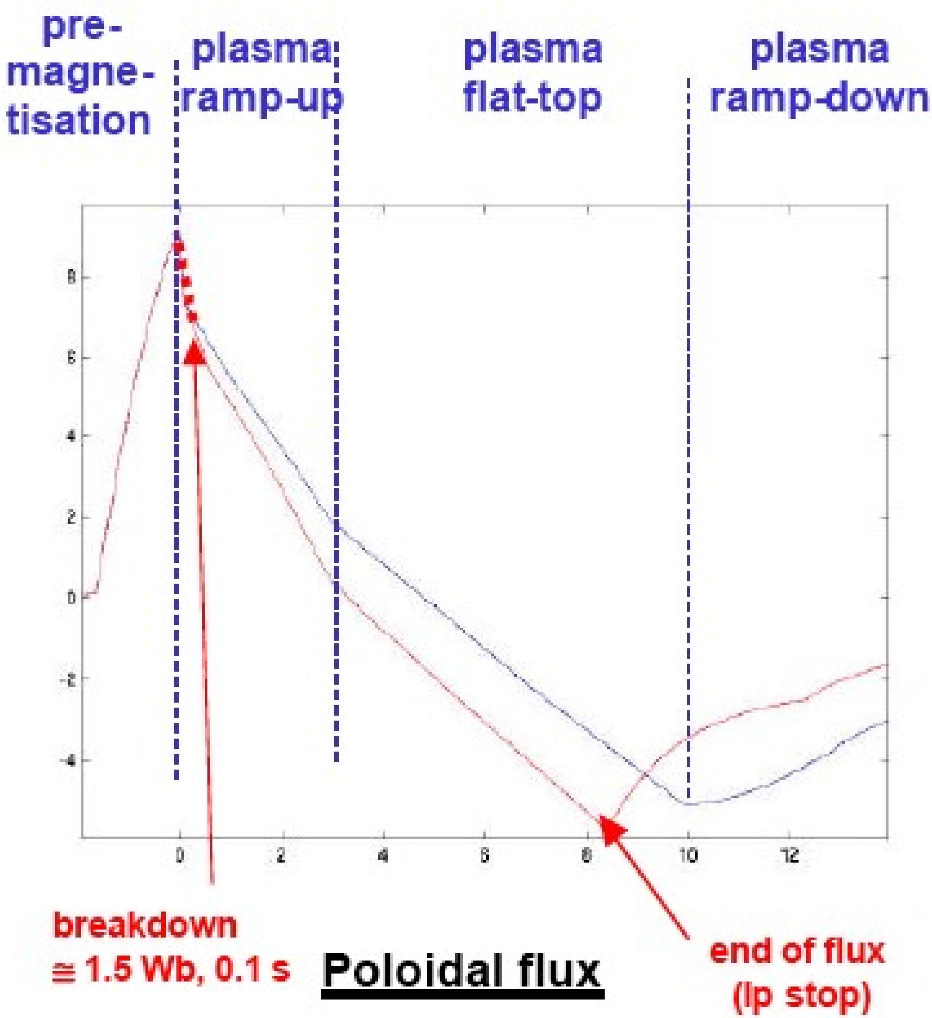

Poloidal flux

ITER conventional scenario

400 MW fusion power
400 s

Fusion power

Plasma current

Inductive flux

DT refuel

Plasma density

He fraction

Additional power

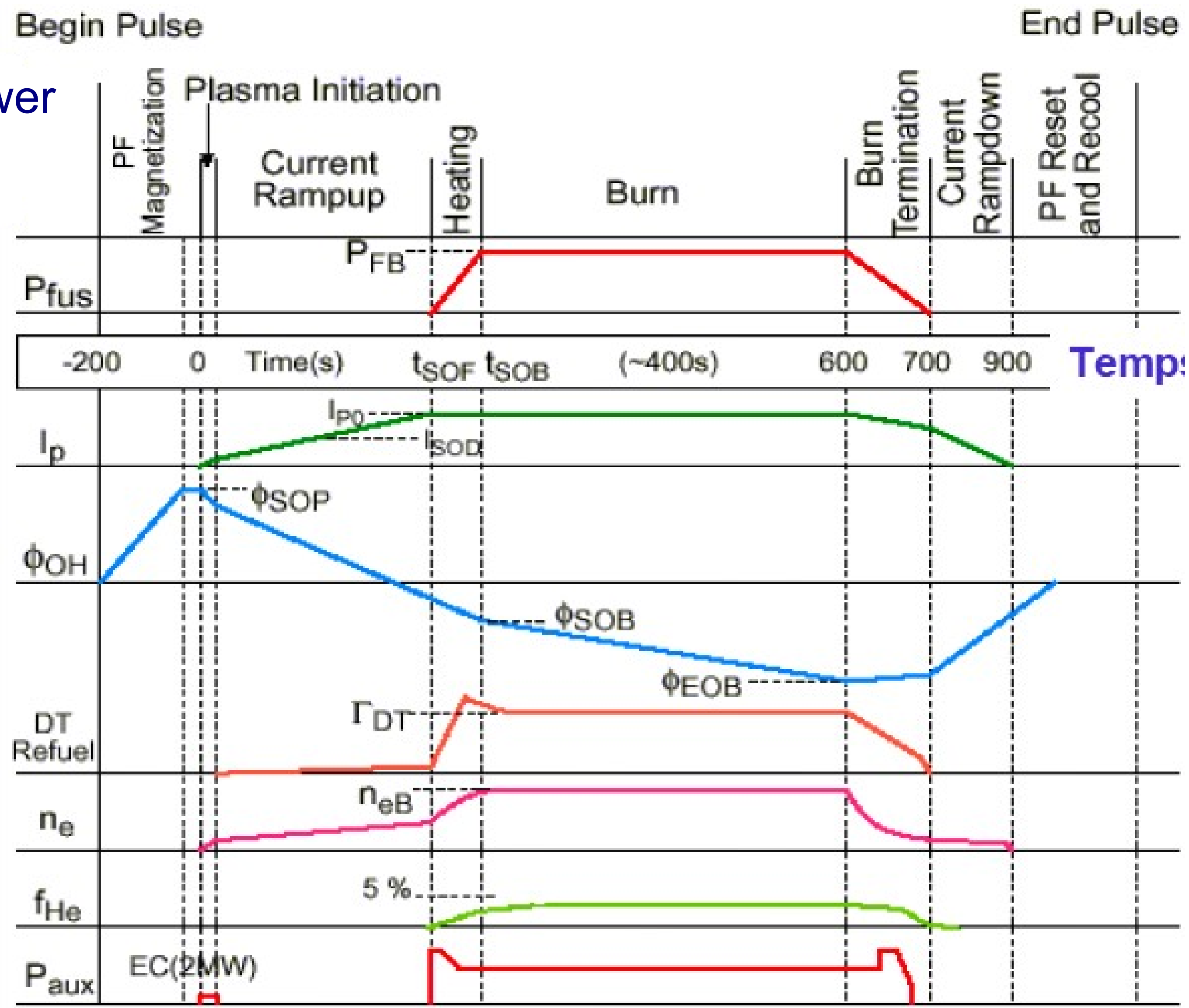

Magnetic measurements

Magnetic measurements

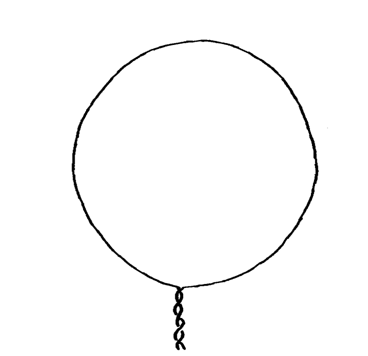

Flux Loop
→ usually one large loop
→ Toroidal **Loop Voltage** measurement
→ **Diamagnetic Loop**

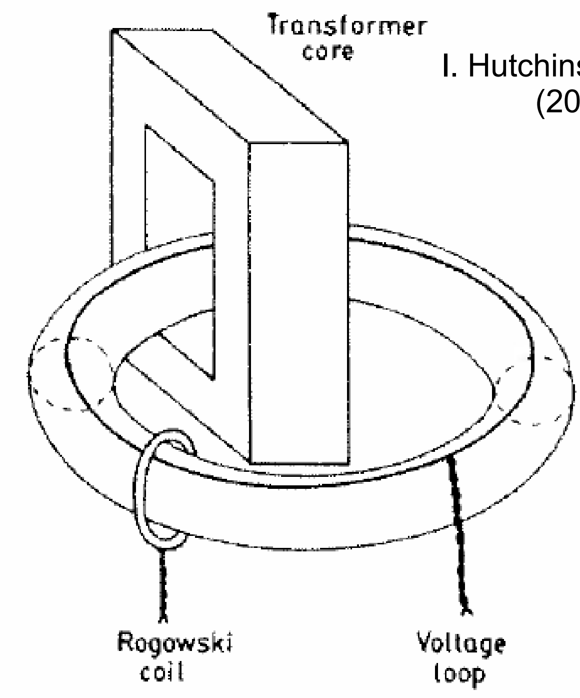

I. Hutchinson (2002)

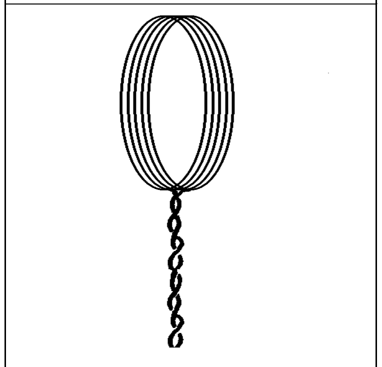

Pick-up coils
→ Small coils
→ Poloidal magnetic component measurements at different locations

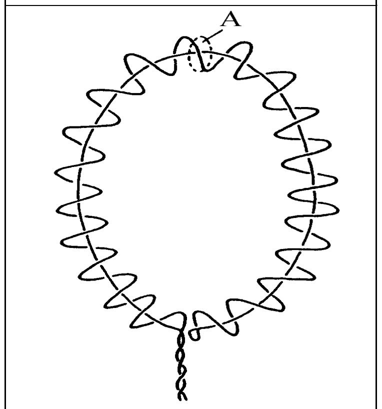

Rogowski coil
→ large non closed coil around the plasma
→ indirect current measurements

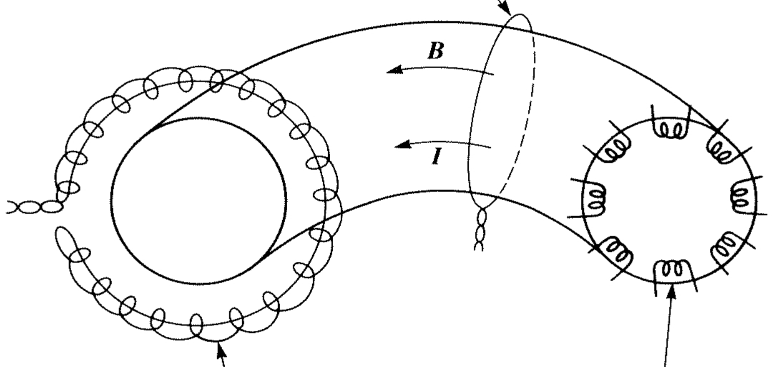

Loop measurements

Maxwell Faraday equation :

$$\vec{\nabla} \wedge \vec{E} = -\frac{\partial B}{\partial t}$$

Stokes theorem :

$$\oint_{\Gamma} \vec{E} . \vec{dl} = \iint \vec{\nabla} \wedge \vec{E} . \vec{ds}$$

Faraday Law :

$$\oint_{\Gamma} \vec{E} . \vec{dl} = -\iint \partial_t \vec{B} . \vec{ds}$$

We will consider magnetic variation slower than electromagnetic waves :

$$kC \gg \omega$$

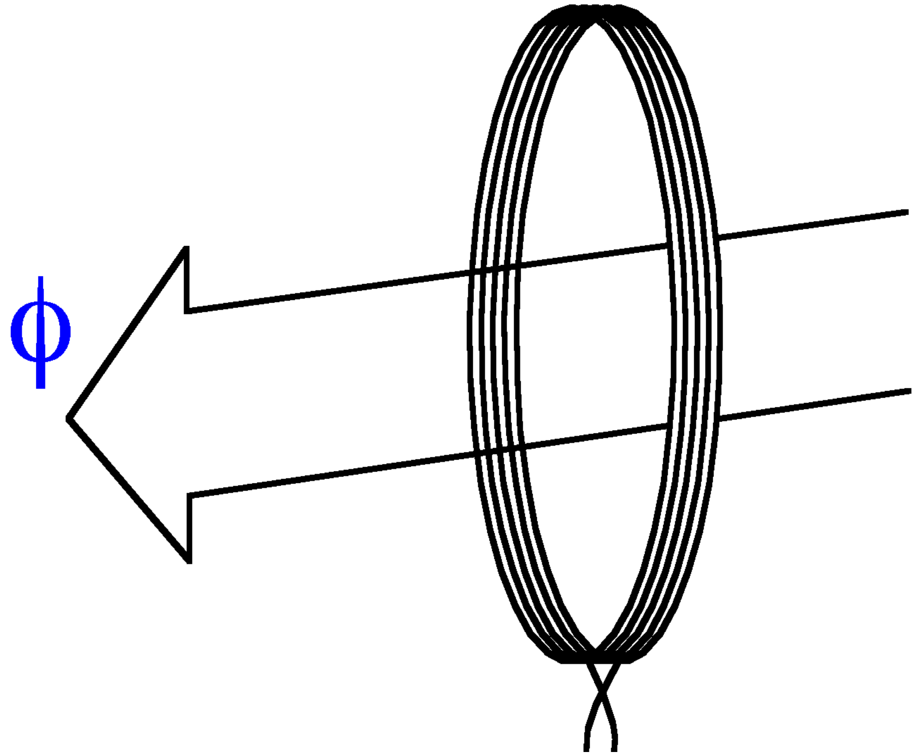

Magnetic flux across the loop :

$$\phi = \iint \vec{B} . \vec{ds}$$

Variation of magnetic flux inside a coil induces a current in a coil :

$$\oint_{\Gamma} \vec{E} . \vec{dl} = -\partial_t \phi$$

Current time integration is needed to deduced magnetic field value at each time

Pick-up coils

N : coil loop number
A : coil loop surface
μ_r : coil internal material relative permeability

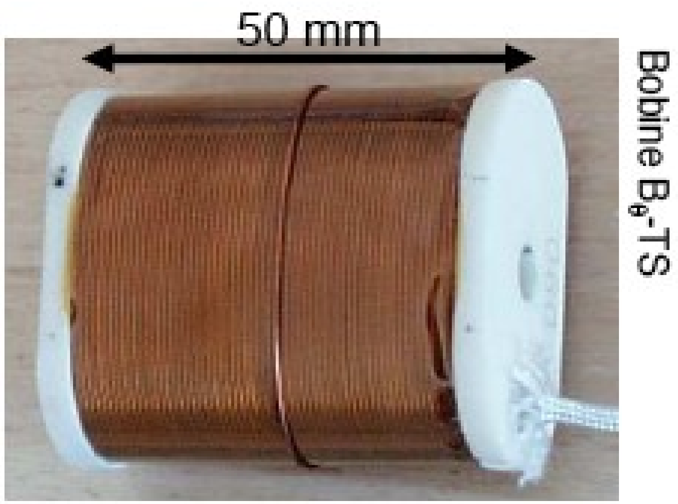

$B(t)$: magnetic **component** along the coil

Coil voltage :

$$V = \mu_r N A \frac{d B(t)}{dt}$$

Magnetic field is obtained by the RC or electronic integrator.

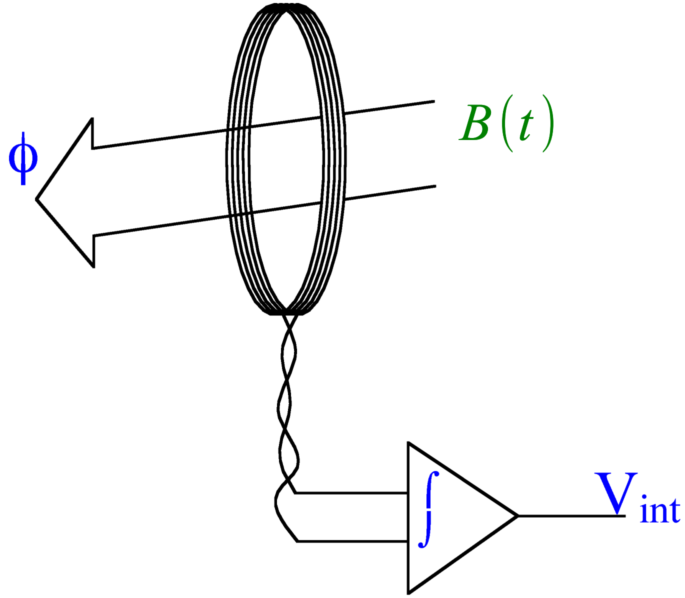

Last Closed Flux Surface position

Example for circular section magnetic surfaces with Shafranov shift.
Poloidal magnetic flux outside the plasma :

$$\psi(r,\theta) = -\frac{\mu_0 R_0 I_\phi}{2\pi}\left(\ln\frac{8R_0}{r} - 2\right) + \frac{\mu_0 I_\phi}{4\pi}\left(1 - \frac{a^2}{r^2}\right)\left(\Lambda + \frac{1}{2}\right) r\cos\theta \qquad \Lambda = \beta_p + \frac{l_i}{2} - 1$$

a_m: pick-up coil small radius
ΔR: plasma radial shift from chamber center
Δz : plasma vertical shift

$\vec{e}_R$: large radius horizontal direction
$\vec{e}_z$: vertical direction

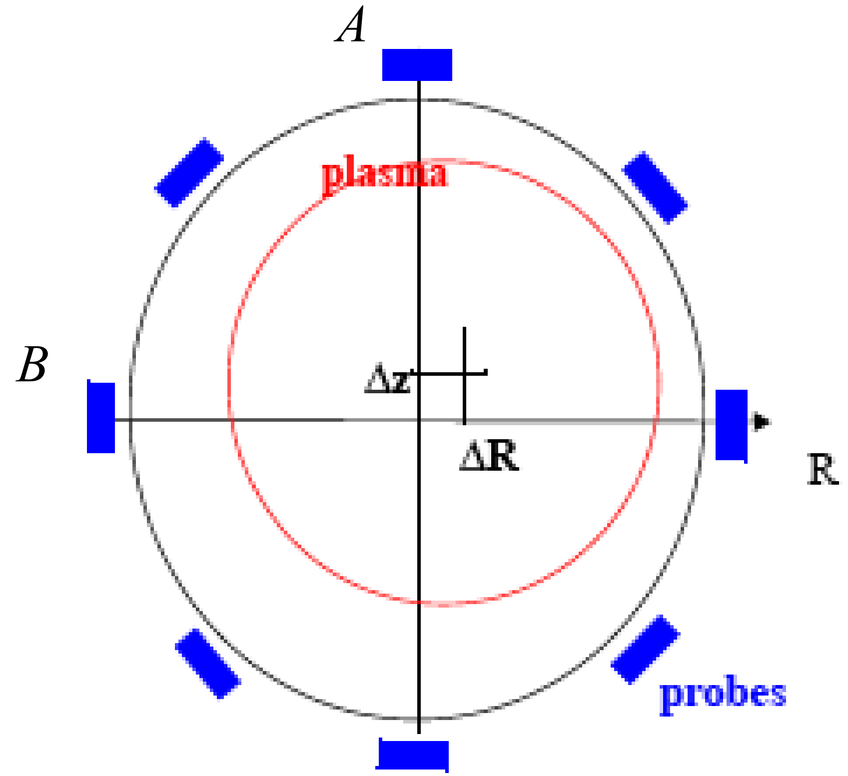

For upper and lower magnetic probes :

$$\oint_\Gamma \vec{B}.\vec{dl} \sim \mu_0 \frac{I_\phi}{2}\frac{\Delta R}{a_m}$$

For left and right magnetic probes :

$$\oint_\Gamma \vec{B}.\vec{dl} \sim \mu_0 \frac{I_\phi}{2}\frac{\Delta z}{a_m}$$

Rogowski Coil

Toroidal plasma current measurement

The coil does make a whole loop around the plasma :

the magnetic flux across the plasma is not included

The coil surrounds the plasma

A : coil cross section area

n : turn number per unit length

The magnetic field varies slowly along the coil :

$$|\nabla B|/B \ll n$$

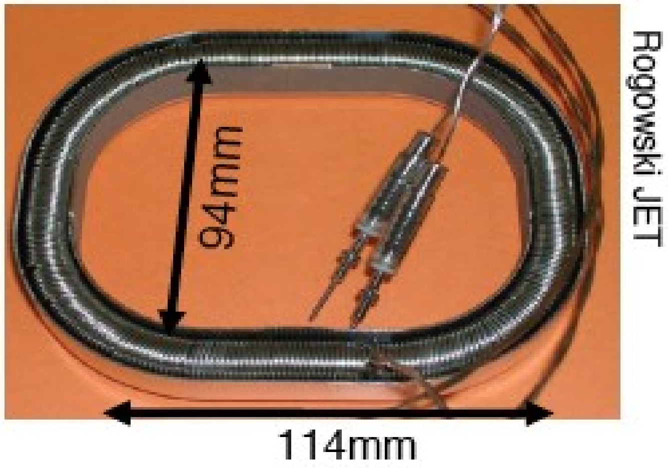

Flux across the coil : $\phi = n \oint_{\Gamma} \iint_{A} ds\, \vec{B}.\vec{dl}$

Ampere's Law : $\oint_{\Gamma} \vec{B}.\vec{dl} = \mu\, I_{\phi}$

$$\phi = n \mu\, A\, I_{\phi}$$

Coil induced voltage :

$$V = \mu\, N\, A \frac{d\, I_{\phi}}{dt}$$

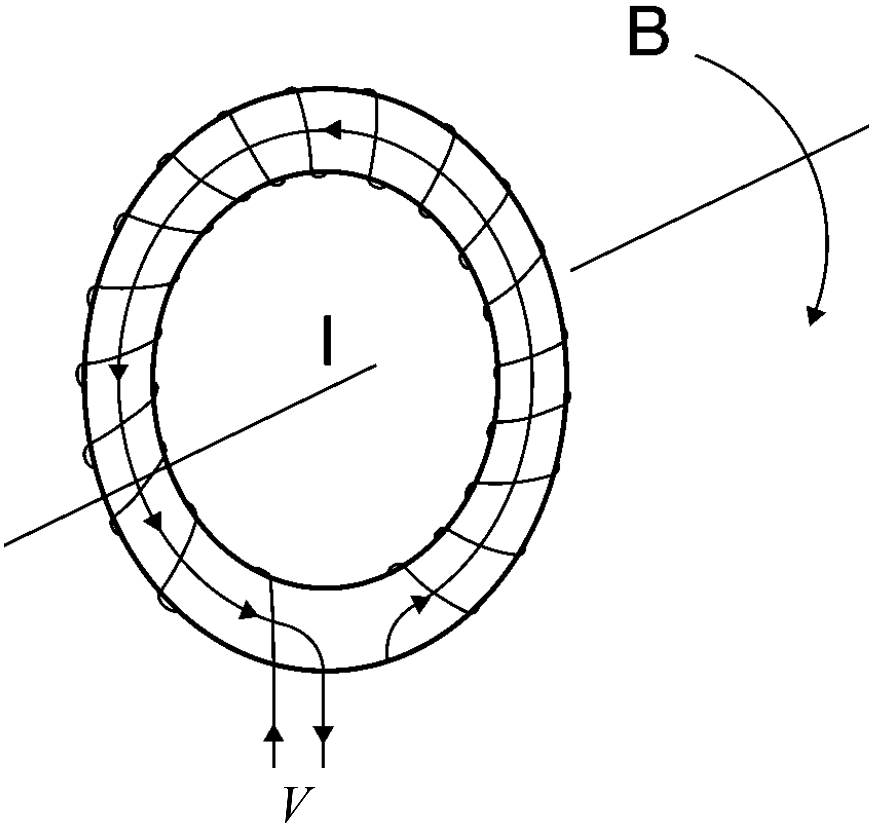

With an additional integrator, the Rogowski coil measures directly the plasma current.

Loop voltage

The loop voltage measures the voltage induced by the **Tokamak transformer** :

$$V = V_\phi$$

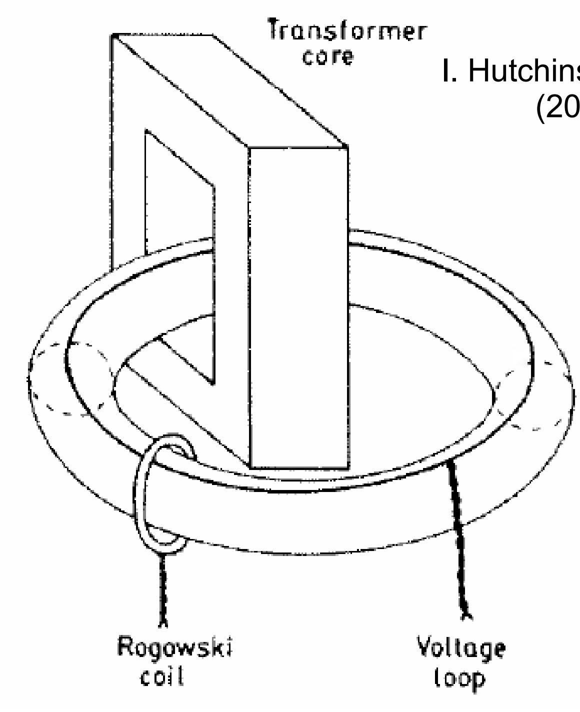

I. Hutchinson (2002)

For stationary plasma ohmic current, the plasma resistance can be directly deduced : $R_P = V_\phi / I_\phi$

The **ohmic heating** power can be deduced : $P_{ohm} = V_\phi I_\phi$

From plasma resistance, electron temperature can be estimated :

Resistance is proportional to the averaged plasma **resistivity** :

$$R_P \sim \eta \frac{2\pi R_0}{\pi a^2}$$

Resistivity is proportional to **collisionality** : $\eta = \dfrac{m_e \nu_{ei}}{q_e^2 n_e}$

ν_{ei} : ion / electron collision frequency

Collisionality is linked to the **electron temperature** : $\nu_{ei} = \dfrac{n_i \ln \Lambda_c}{3\pi^{3/2} \epsilon_0^2} \dfrac{m_e^{1/2} Z_i^2 q_e^4}{m_i (k_B T_e)^{3/2}}$

(Coulomb collisions)

This property was used to evaluate the electron temperature inside first Tokamaks (600 eV on T3 tokamak).

Diamagnetic loop

Diamagnetism : B_ϕ is modified by the presence of the kinetic pressure P .

The diamagnetic loop allows to measure the plasma integrated B_ϕ .

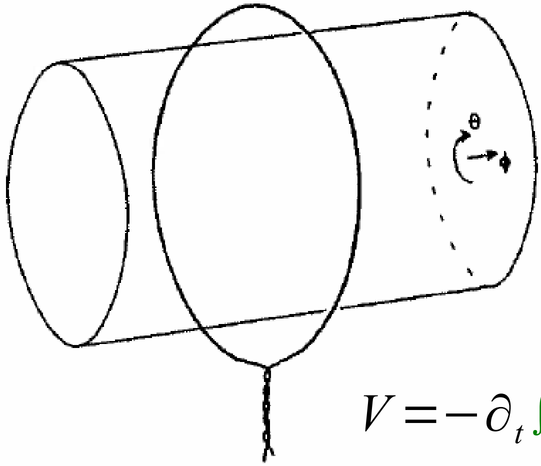

I. Hutchinson (2002)

$$V = -\partial_t \iint_{r\theta} B_\phi$$

We consider large aspect ratio tokamak : B_ϕ variation with R is neglected to put forward kinetic pressure effect on magnetic field.
Plasma pressure equilibrium across the plasma :

$$\left[\vec{\nabla}_\perp \left(P + \frac{B^2}{2\mu_0}\right) - \frac{B^2}{2\mu_0}\vec{k}_B\right] . \vec{e}_r = 0$$

$$\frac{dP}{dr} + \frac{B_\phi}{\mu_0}\frac{dB_\phi}{dr} + \frac{1}{r}\frac{B_\theta}{\mu_0}\frac{d(r B_\theta)}{dr} = 0$$

Multiplied by r^2 and integrated from 0 to a (where $P_a = 0$) :

The plasma average kinetic pressure only function of the magnetic fields :

$$\langle P \rangle_{r\theta} = \frac{B_{\theta a}^2 + B_{\phi a}^2 - \langle B_\phi^2 \rangle_{r\theta}}{2\mu_0}$$

$\langle ... \rangle_{r\theta}$: poloidal section average

Diamagnetic loop

$$\langle P \rangle_{r\theta} = \frac{B_{\theta a}^2 + B_{\phi a}^2 - \langle B_\phi^2 \rangle_{r\theta}}{2\mu_0}$$

β_θ and β_ϕ are defined from separated magnetic field components:

$$\beta_\theta = \frac{2\mu_0 \langle P \rangle_{r\theta}}{B_{\theta a}^2} = \frac{B_{\theta a}^2 + B_{\phi a}^2 - \langle B_\phi^2 \rangle_{r\theta}}{B_{\theta a}^2}$$

Since $\beta_\phi = 2\mu_0 \langle P \rangle_{r\theta} / B_\phi^2 \ll 1$ and $B_\theta \ll B_\phi$,
B_ϕ has small variations across the plasma : $\langle B_\phi \rangle_{r\theta} - B_{\phi a} \ll B_{\phi a}$

$$\langle B_\phi^2 \rangle_{r\theta} - B_{\phi a}^2 \sim 2 B_{\phi a} \left(\langle B_\phi \rangle_{r\theta} - B_{\phi a} \right)$$

Hence : $\beta_\theta = 1 + \dfrac{2 B_{\phi a} \left(B_{\phi a} - \langle B_\phi \rangle_{r\theta} \right)}{B_{\theta a}^2}$

$$\beta_\phi = \frac{2\mu_0 \langle P \rangle_{r\theta}}{B_{\phi a}^2} = \frac{B_{\theta a}^2 + B_{\phi a}^2 - \langle B_\phi^2 \rangle_{r\theta}}{B_{\phi a}^2}$$

Since $B_\theta \ll B_{\phi a}$: $\beta_\phi = \dfrac{2 B_{\phi a} \left(B_{\phi a} - \langle B_\phi \rangle_{r\theta} \right)}{B_{\phi a}^2}$

Since $\beta_\phi > 0$, $\langle B_\phi \rangle_{r\theta} < B_{\phi a}$, the Tokamak plasma is diamagnetic.

Plasma main properties

$$\langle P \rangle_{r\theta} = \frac{B_{\theta a}^2 + B_{\phi a}^2 - \langle B_\phi^2 \rangle_{r\theta}}{2\mu_0}$$

$B_{\phi a}$ and $B_{\theta a}$ are measured by plasma edge pick-up coils.
$\langle B_\phi \rangle_{r\theta}$ is measured by **poloidal diamagnetic** loop.

$\langle B_\phi \rangle_{r\theta}$ measurements is difficult : B_ϕ diamagnetic variation when plasma occurs is of the order of 10^{-3} .

Magnetic measurements allow the plasma kinetic pressure evaluation.

the plasma kinetic energy evaluation :

$$W = \frac{3}{2} 2\pi R_0 \pi a^2 \langle P \rangle_{r\theta}$$

and the energy confinement time for **ohmic** plasmas :

$$\tau_E = \frac{W}{P_{ohm}}$$

$$P_{ohm} = V_\phi I_\phi$$

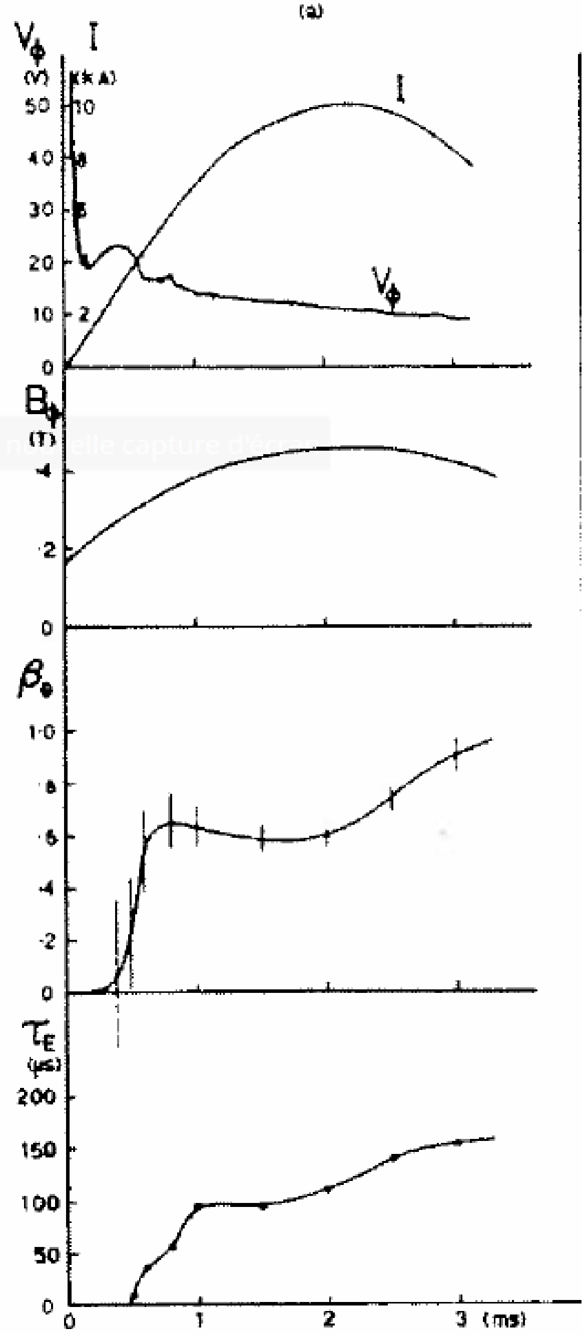

I. Hutchinson Pl.Ph. (1976)

Tore supra magnetic measurements

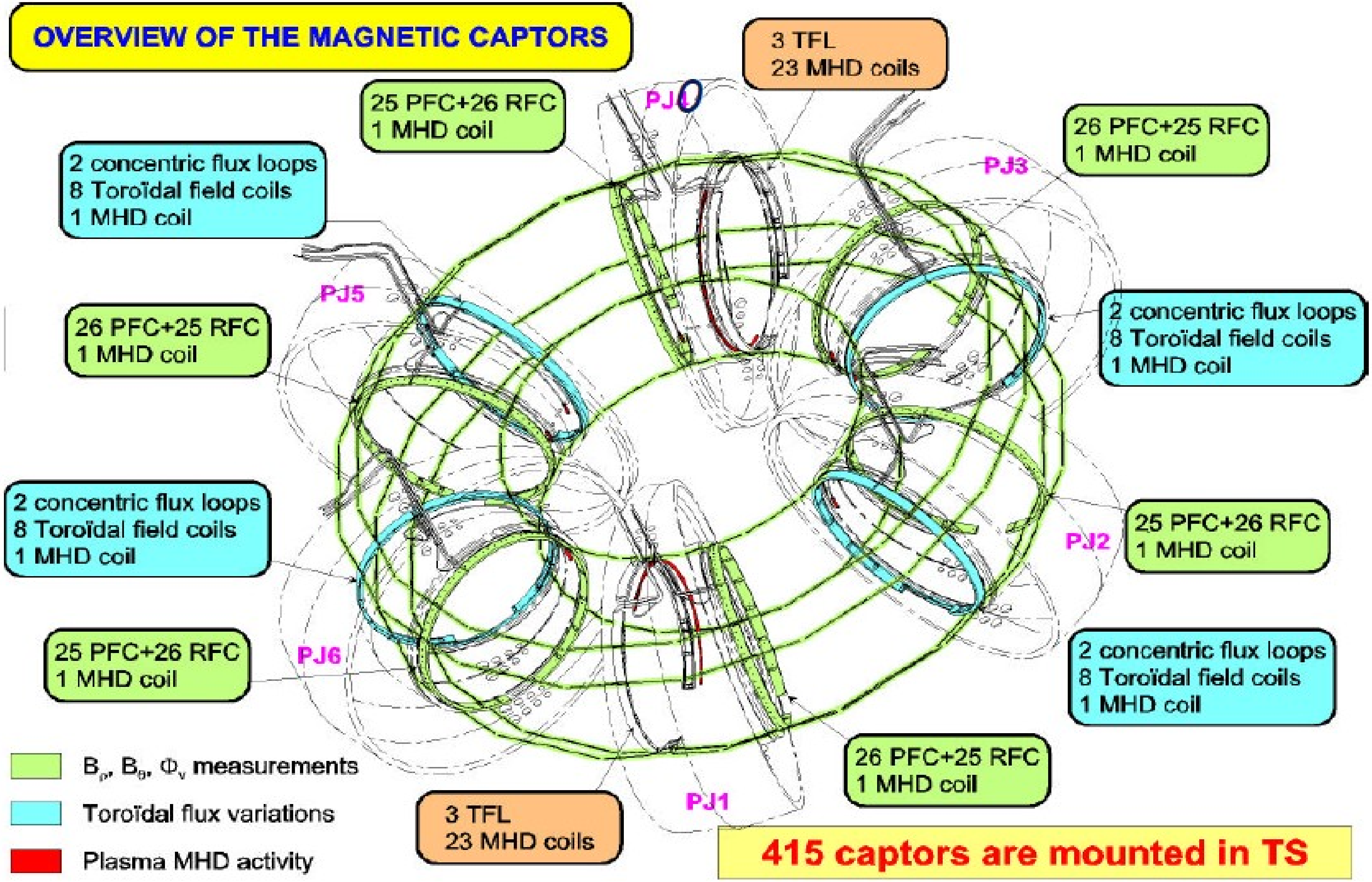

WEST magnetic measurements

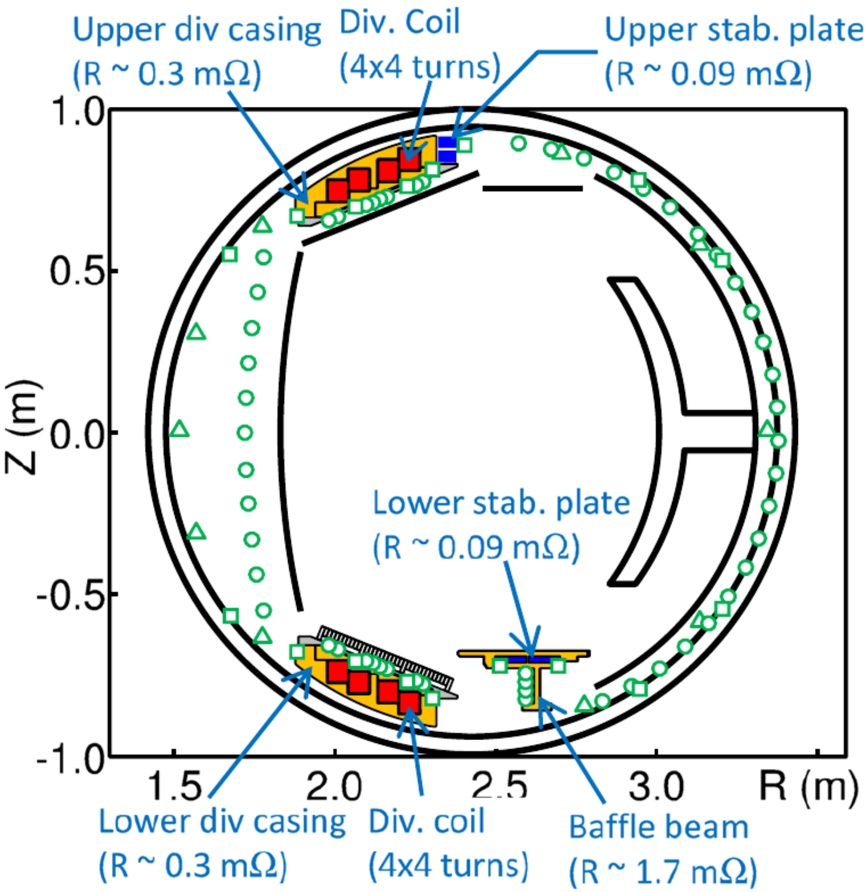

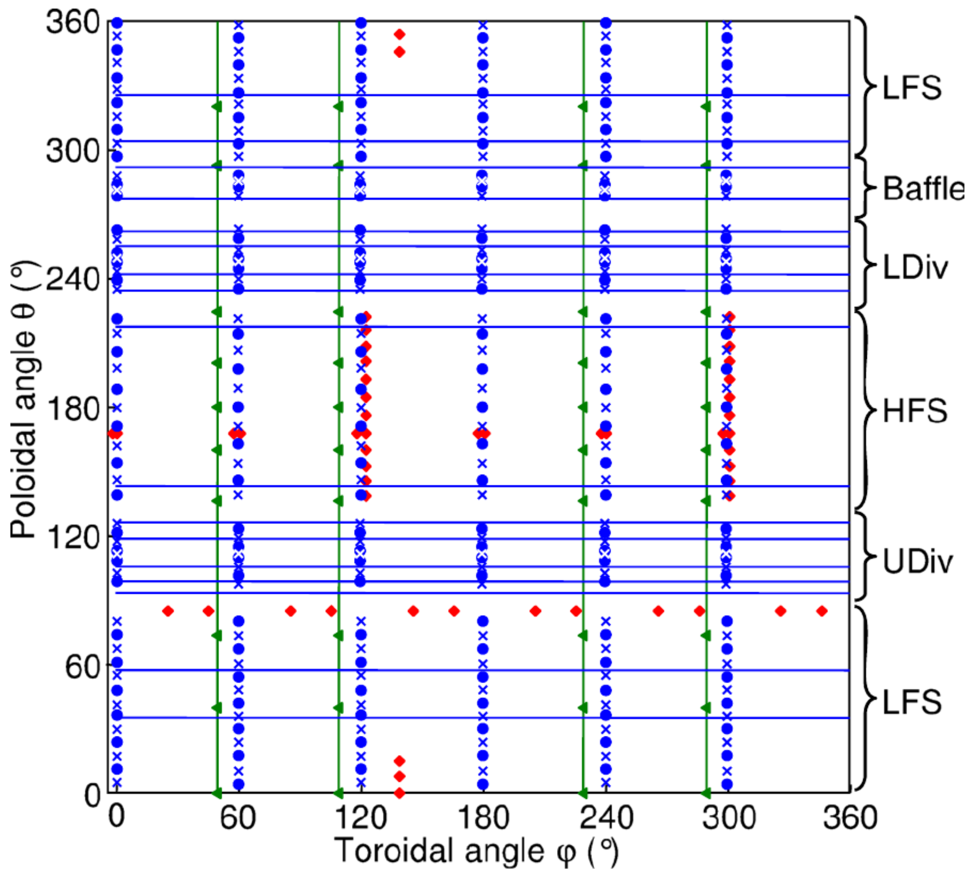

- divertor coils
- copper stabilizing plates
- toroidally continuous support structures.
- tangential and normal field probes
- toroidal field probes
- flux loops

- x tangential field probes,
- normal field probes
- toroidal field probes
- high frequency sensors
- toroidal flux loops
- diamagnetic flux loops

P. Moreau, RSI (2018)

Interfero-Polarimetry

Refractive index measurements : wave propagation

Electromagnetic wave propagation inside a plasma.
The wave is monochromatic : ω_i
The wave is transverse linear mono-mode :

$$\vec{E}_i(\vec{r},t)=e^{i(\vec{k}_i.\vec{r}-\omega_i t)}\vec{E}_{i0}$$

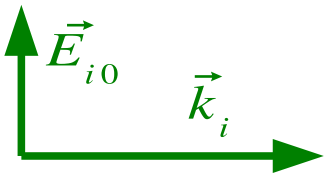

The plasma is a lossless linear non-dispersive magneto-active medium

Wave equation : $$\vec{\nabla}^2\vec{E}_i(\vec{r},t)-\frac{n_{OX}^2}{C^2}\frac{\partial^2}{\partial t^2}\vec{E}_i(\vec{r},t)=0$$

n_{OX} is the refractive index:

$$n_{OX}=C\frac{k_i}{\omega_i}$$

The refractive index differs if the wave polarization is parallel (O mode) or perpendicular (X mode) to the magnetic field.

Propagation perpendicular to the magnetic field

Propagation perpendicular to the magnetic field
Cold plasma approximation

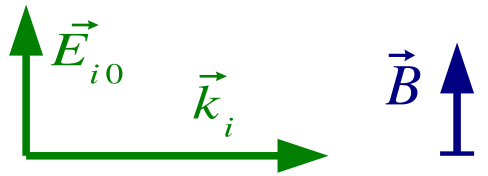

Wave electric field parallel to the magnetic field (O mode) :

$$n_O = \sqrt{1 - \frac{\omega_p^2}{\omega_i^2}} \qquad \omega_p = \sqrt{\frac{q_e^2 n_e}{\varepsilon_0 m_e}}$$

Wave electric field perpendicular to the magnetic field (X mode) :

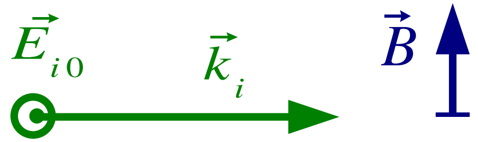

$$n_X = \sqrt{\frac{RL}{S}}$$

$$R = 1 - \frac{\omega_p^2}{\omega_i(\omega_i + \omega_{ce})} \qquad L = 1 - \frac{\omega_p^2}{\omega_i(\omega_i - \omega_{ce})} \qquad S = \frac{(R+L)}{2} \qquad \omega_{ce} = \frac{q_e B}{m_e}$$

When $\omega_i \gg \omega_p$ and $\omega_i \gg \omega_{ce}$: $R \sim L \sim S \sim 1 - \frac{\omega_p^2}{\omega_i^2}$

$$\boxed{n_O \sim n_X \sim 1 - \frac{\omega_p^2}{2\,\omega_i^2} = 1 - \frac{n_e}{2\,n_{cr}}} \qquad n_{cr} = \omega_i^2 \frac{m_e \epsilon_0}{q_e^2} \qquad n_{cr} \gg n_e$$

High frequency electromagnetic wave propagates like in a non magneto-active plasma.

Interferometry

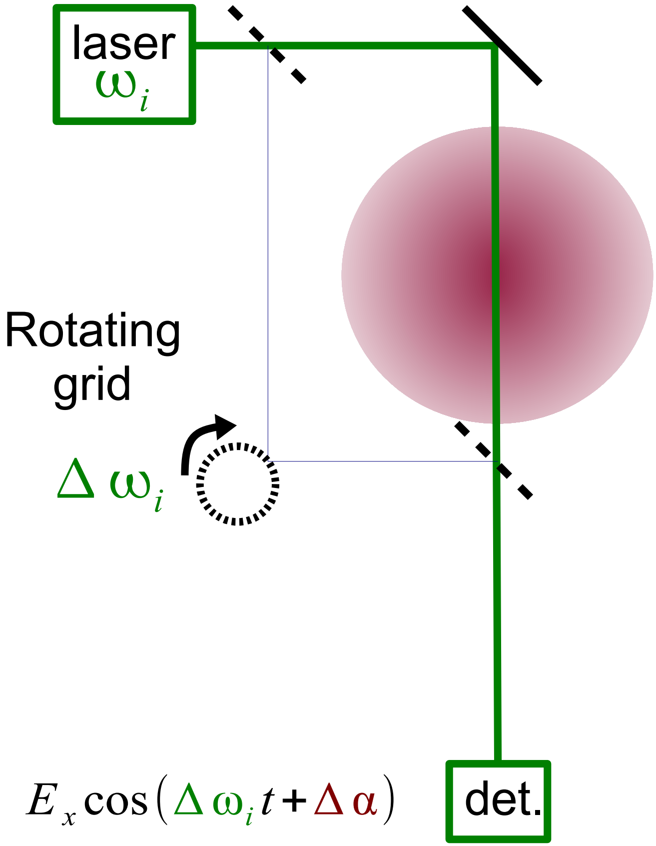

Mach-Zehnder interferometer configuration :

A laser beam is sent through the plasma

It interferes with a reference beam with the same propagation distance outside the plasma.

Because of the propagation inside the plasma, there is a **phase shift** between both beams :

$$\Delta\alpha = \int (k(z) - k_i)\, dz = \frac{\omega_i}{C} \int (n_O(z) - 1)\, dz$$

$$k(z) = k_i n_O(z)$$

$$k_i = \frac{\omega_i}{C}$$

For laser light : $\omega_i \gg \omega_c \quad \omega_i \gg \omega_p$

$$n_O \sim 1 - \tfrac{1}{2} n_e / n_{cr}$$

The phase shift is proportional to the density integrated along the beam chord across the plasma :

$$n_l = \int n_e(z)\, dz$$

$$\boxed{\Delta\alpha = \frac{-\omega_i}{2 C n_{cr}} \int n_e(z)\, dz = \frac{-\omega_i}{2 C n_{cr}} n_l}$$

Because of the **rotating grid** placed on the reference beam, the interference between the reference and the beam through plasma is shifted in frequency and is so easier to detect.

Propagation parallel to the magnetic field (Faraday rotation)

Propagation of a linear electromagnetic wave parallel to the magnetic field

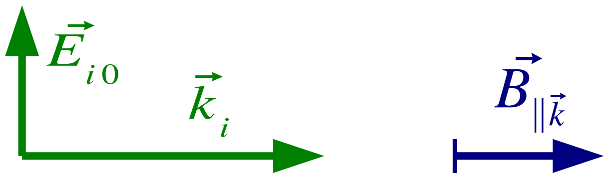

The Eigenmodes are circular modes (Left and Right) with different refractive index :

$$n_R = \sqrt{R} = \sqrt{1 - \frac{\omega_p^2}{\omega_i(\omega_i + \omega_{ce})}} \qquad n_L = \sqrt{L} = \sqrt{1 - \frac{\omega_p^2}{\omega_i(\omega_i - \omega_{ce})}}$$

The linear mode is a superposition of both circular modes.
Since both circular modes have slightly different refractive indices, the linear polarization is rotating along propagation :

$$\frac{d\alpha_F}{dz} = \frac{1}{2}(n_R - n_L)\frac{\omega_i}{C}$$

When : $\omega_i \gg \omega_p \qquad \omega_i \gg \omega_{ce}$

$$\frac{d\alpha_F}{dz} \sim \frac{\omega_p^2 \omega_{ce}}{2C\omega_i^2} = \frac{q_e}{2m_e C}\frac{n_e}{n_c}B_{\parallel \vec{k}}$$

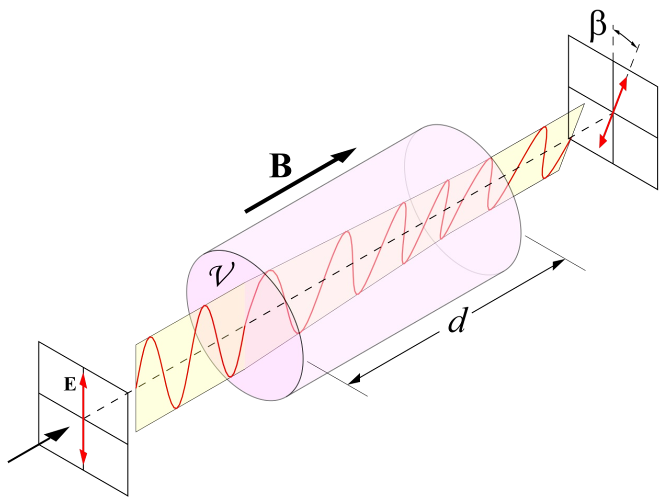

Polarimetry

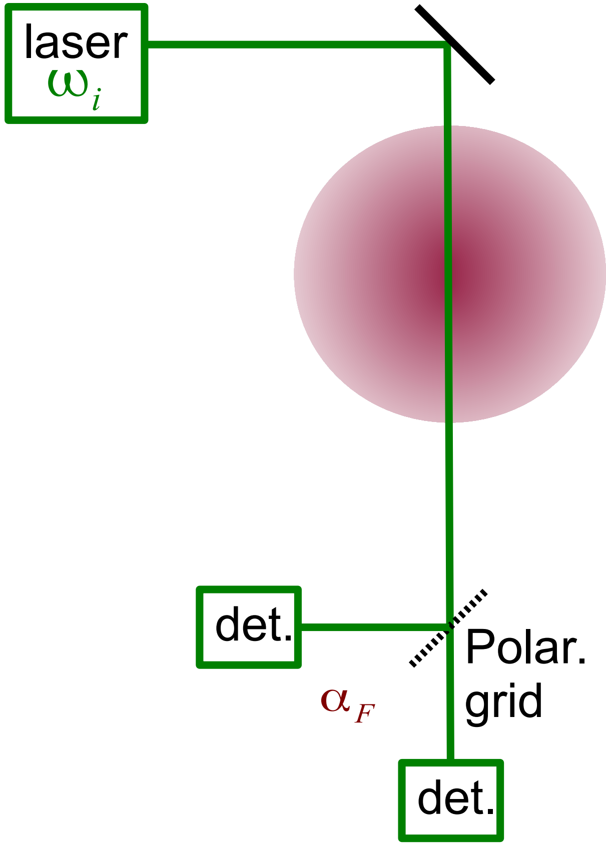

Polarimetry :
The Faraday rotation inside the plasma of a laser beam polarization is a linear integration along the laser chord inside the plasma.
When $\omega_i \gg \omega_p$ $\omega_i \gg \omega_{ce}$

$$\boxed{\alpha_F \sim \frac{q_e}{2 m_e C} \int \frac{n_e(z)}{n_c} \vec{B}(z) . \vec{dz}}$$

To measure Faraday rotation of the laser beam inside the plasma, a polarization grid is placed in front of the detector to separate both linear polarization.

Interfero-Polarimetry

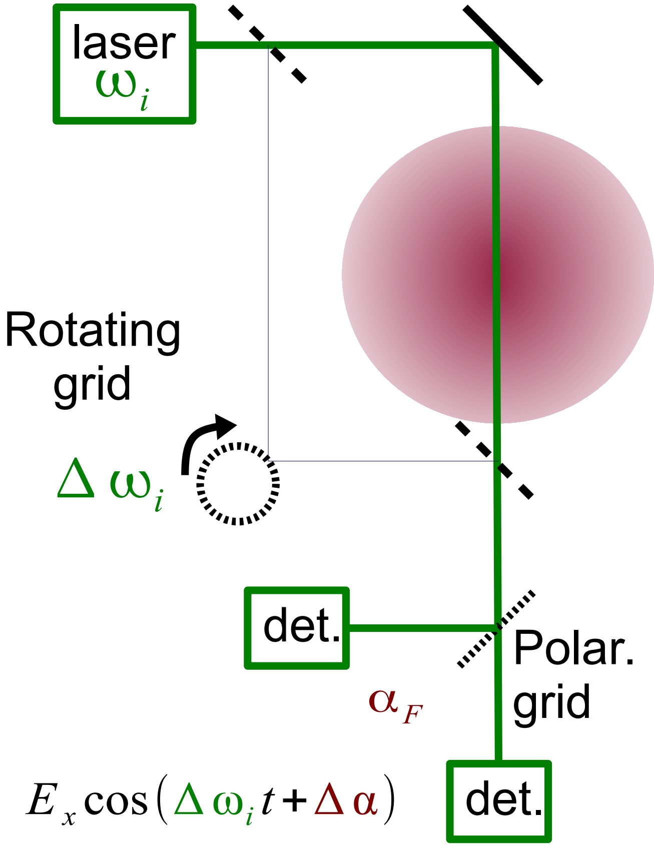

Both diagnostics are combined in a single optical bench.

Interferometry measurements are complicated to due the size of the Tokamak plasma and the coherence limit length of the laser beams.

2 lasers with different wavelengths are combined to reduce noise for interferometry measurements.

Interfero-Polarimetry on WEST

8 horizontal chords
2 transverse chords
2 lasers FIR CW :
DCN (195 µm, 150 mW)
H_2O (119 µm, 35 mW)
Rotating grid frequency : 100 kHz

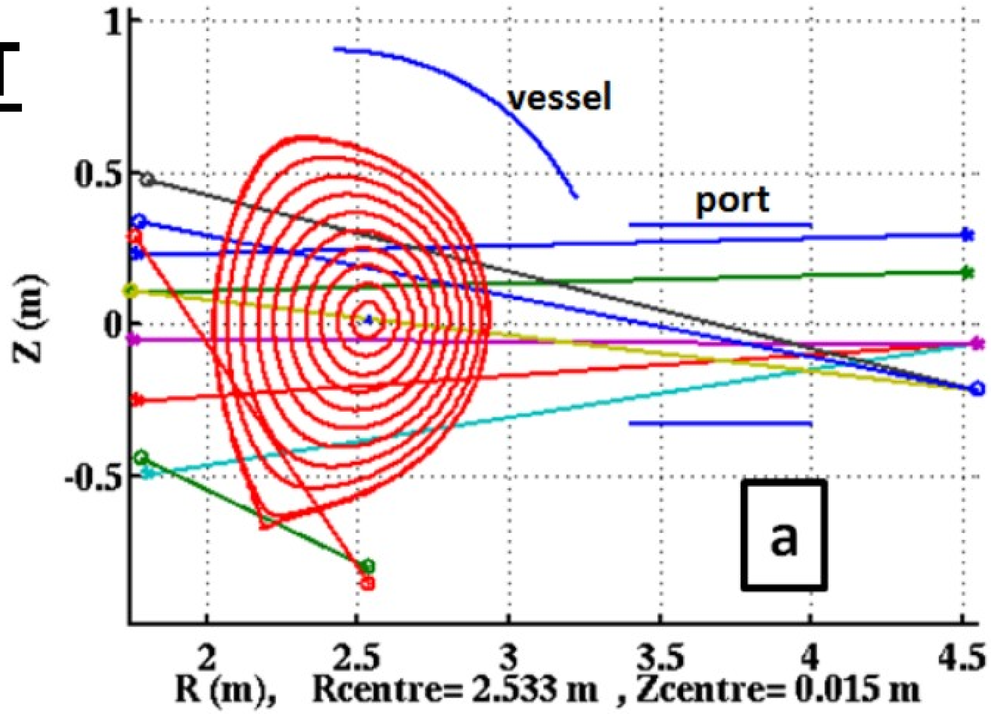

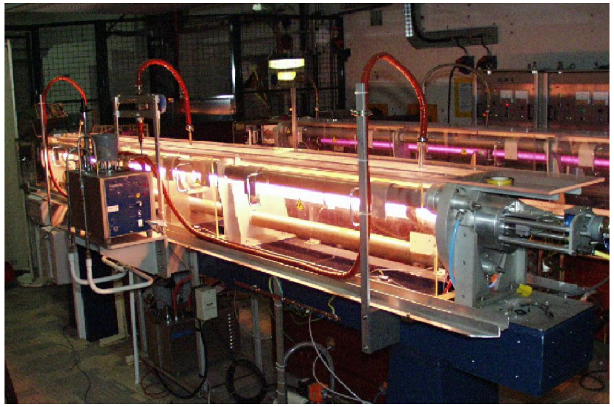

Lineic density and
Faraday angle signals :
1 ms resolution
real time

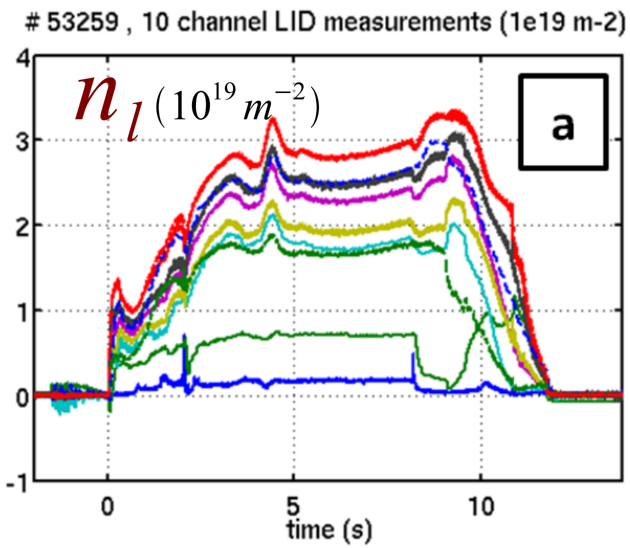

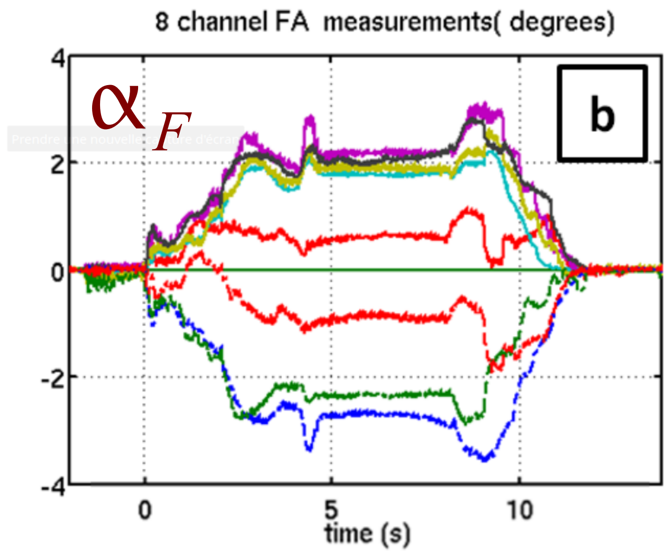

C. Gil, Hal-CEA (2019)

MHD Equilibrium reconstruction

MHD Equilibrium reconstruction

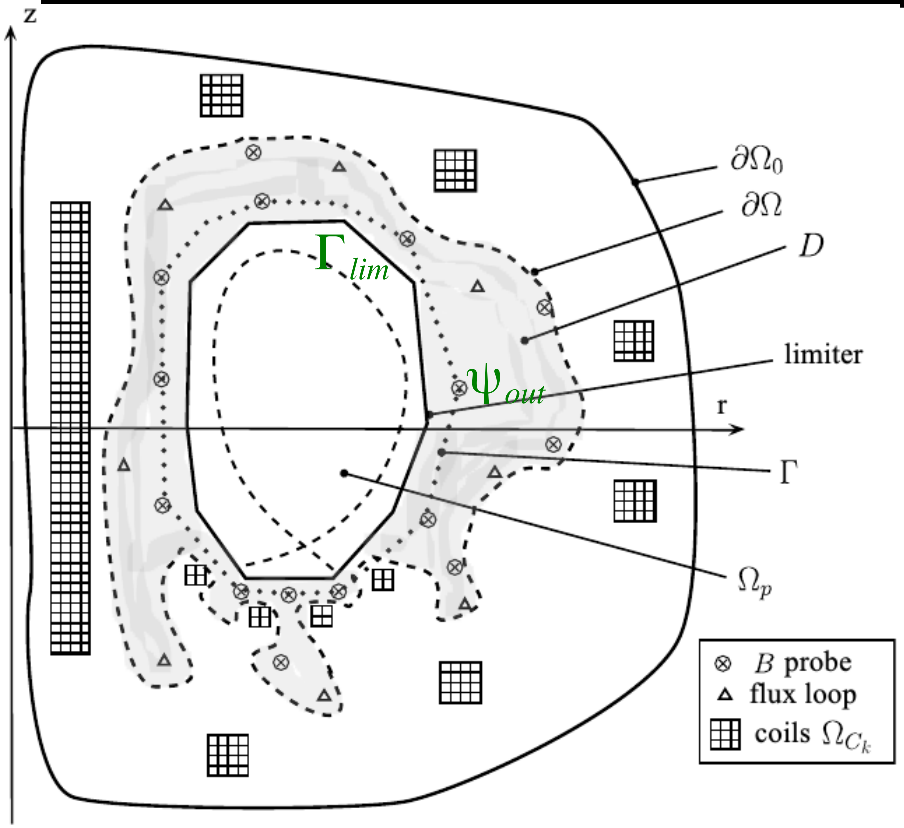

B. Faugeras, J. Blum, PPCF (2014)

Grad-Shafranov equation in the outer domain D between
- the plasma (fixed boundary: the plasma limiter)
- and the external coils:

$$R\frac{\partial}{\partial R}\frac{1}{R}\frac{\partial\psi_{out}}{\partial R}+\frac{\partial^2\psi_{out}}{\partial z^2}=0$$

Using toroidal harmonics to do interpolations and extrapolations of magnetic measurements in the annular domain D.

A reduced number of harmonics is used

Bipolar coordinates (ζ,η) Poles $(\pm R_0, z_0)$

$$R=\frac{R_0\sinh\zeta}{\sqrt{\cosh\zeta-\cos\eta}}$$

$$z-z_0=\frac{R_0\sin\eta}{\sqrt{\cosh\zeta-\cos\eta}}$$

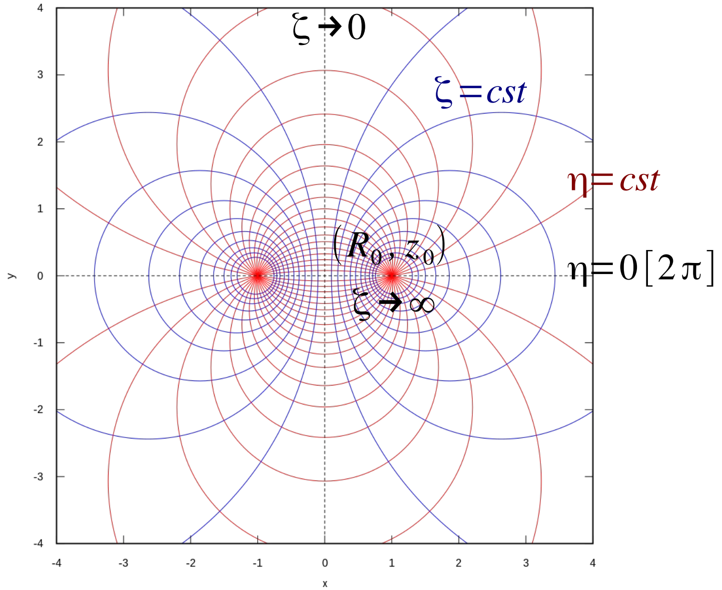

MHD Equilibrium reconstruction (NICE)

Solutions: $\psi_{out} = \psi_{out\,i} + \psi_{out\,e}$

$$\psi_i(\zeta,\eta) = \frac{R_0 \sinh\zeta}{\sqrt{\cosh\zeta - \cos\eta}} \left[\sum_{n=0}^{+\infty} a_n^i P_{n-1/2}^1(\cosh\zeta)\cos n\eta + \sum_{n=0}^{+\infty} b_n^i P_{n-1/2}^1(\cosh\zeta)\sin n\eta\right]$$

$$\psi_e(\zeta,\eta) = \frac{R_0 \sinh\zeta}{\sqrt{\cosh\zeta - \cos\eta}} \left[\sum_{n=0}^{+\infty} a_n^e Q_{n-1/2}^1(\cosh\zeta)\cos n\eta + \sum_{n=0}^{+\infty} b_n^e Q_{n-1/2}^1(\cosh\zeta)\sin n\eta\right]$$

$P_{n-1/2}^1$
$Q_{n-1/2}^1$ 1st and 2nd kind Legendre functions

$\psi_{out\,i}$ solutions with internal plasma current $\lim_{\zeta\to\infty} P_{n-1/2}^1(\cosh\zeta) \rightarrow \textit{singularity near poles}$

$\psi_{out\,e}$ solutions with external coil currents $\lim_{\zeta\to 0} Q_{n-1/2}^1(\cosh\zeta) \rightarrow \textit{singularity near tokamak axis}$

Truncated solution:
$(a_0^i, \dots, a_{n_{ai}}^i, a_0^e, \dots, a_{n_{ae}}^e, b_0^i, \dots, b_{n_{bi}}^i, b_0^e, \dots, b_{n_{be}}^e)$ unknowns

Numerical solution using all the magnetic measurements in the outside domain.
Least mean square method is used to evaluate the difference.

This solution in this outer domain gives the solution for the plasma limiter boundary Γ_{lim}:

$$\psi_{\Gamma_{lim}} \qquad \vec{B}_{\Gamma_{lim}}$$

MHD Equilibrium reconstruction (EQUINOX)

Grad-Shafranov equation inside the limiter :

$$R\frac{\partial}{\partial R}\frac{1}{R}\frac{\partial \psi_{in}}{\partial R}+\frac{\partial^2 \psi_{in}}{\partial z^2}=-\mu_0 R^2\frac{dP}{d\psi_{in}}-\mu_0^2 I_{r\theta}\frac{dI_{r\theta}}{d\psi_{in}}$$

Solution on the limiter Γ_{lim} is known :

$$\psi_{in}=\psi_{\Gamma_{lim}} \qquad \vec{B}_{in}=\vec{B}_{\Gamma_{lim}}$$

Is it possible to determine $P(\psi)$ and $I_{r\theta}(\psi)$ knowing $\psi_{\Gamma_{lim}}$ and $\vec{B}_{\Gamma_{lim}}$ (with or without polarimetry)?

For the circular and large aspect ratio case :

$$B_\theta(a)=B_{\theta 0}(a)\left[1+\frac{a}{R_0}(\beta_p+\frac{1}{2}l_i-1)\cos\theta\right]$$

The solution gives only the sum $\beta_p+\frac{1}{2}l_i$.

For less smooth geometries, it is possible to approach $P(\psi)$ and $I_\theta(\psi)$ profiles.

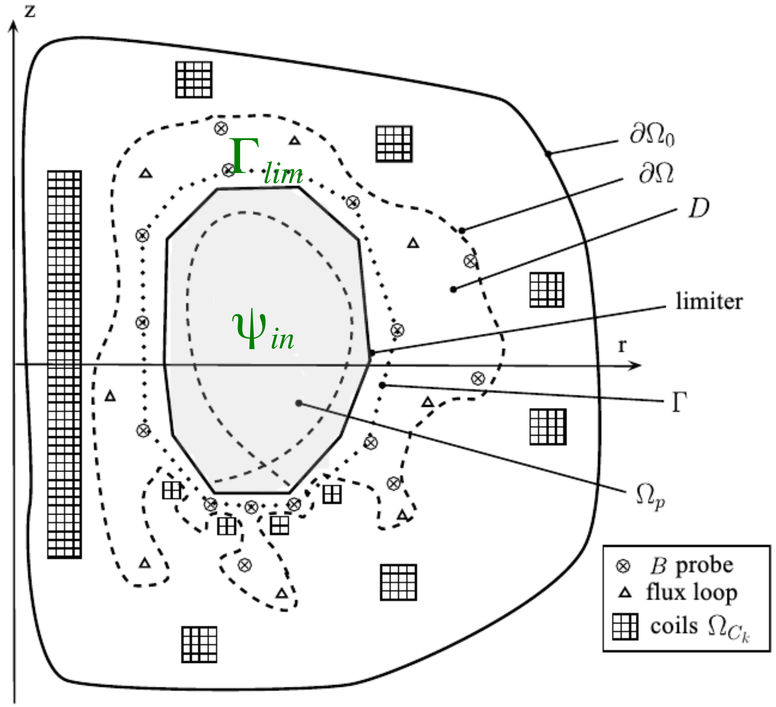

Equilibrium reconstruction : Tore Supra

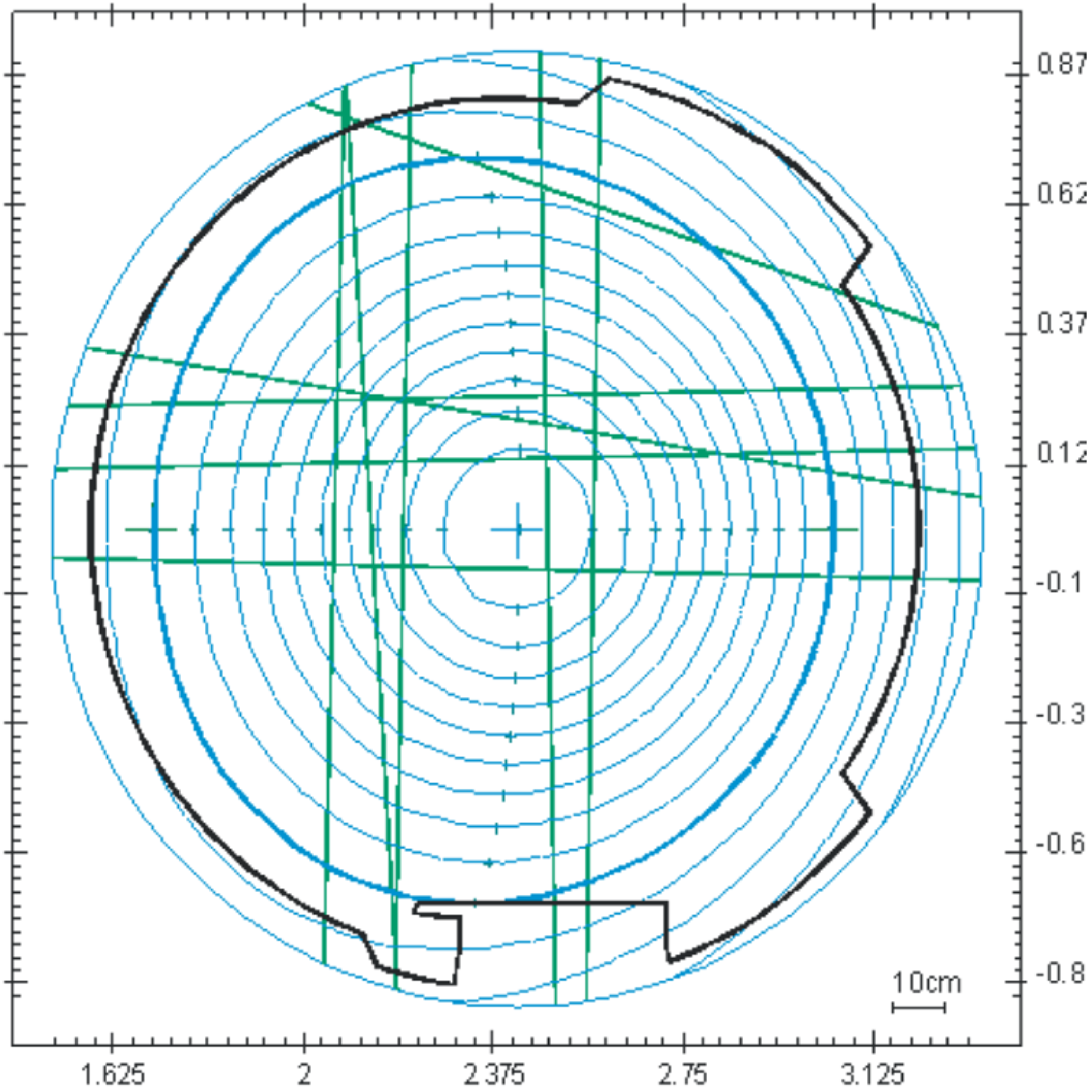

B. Faugeras, GT Plasma (2012)

Equilibrium reconstruction : Tore Supra (limiter)

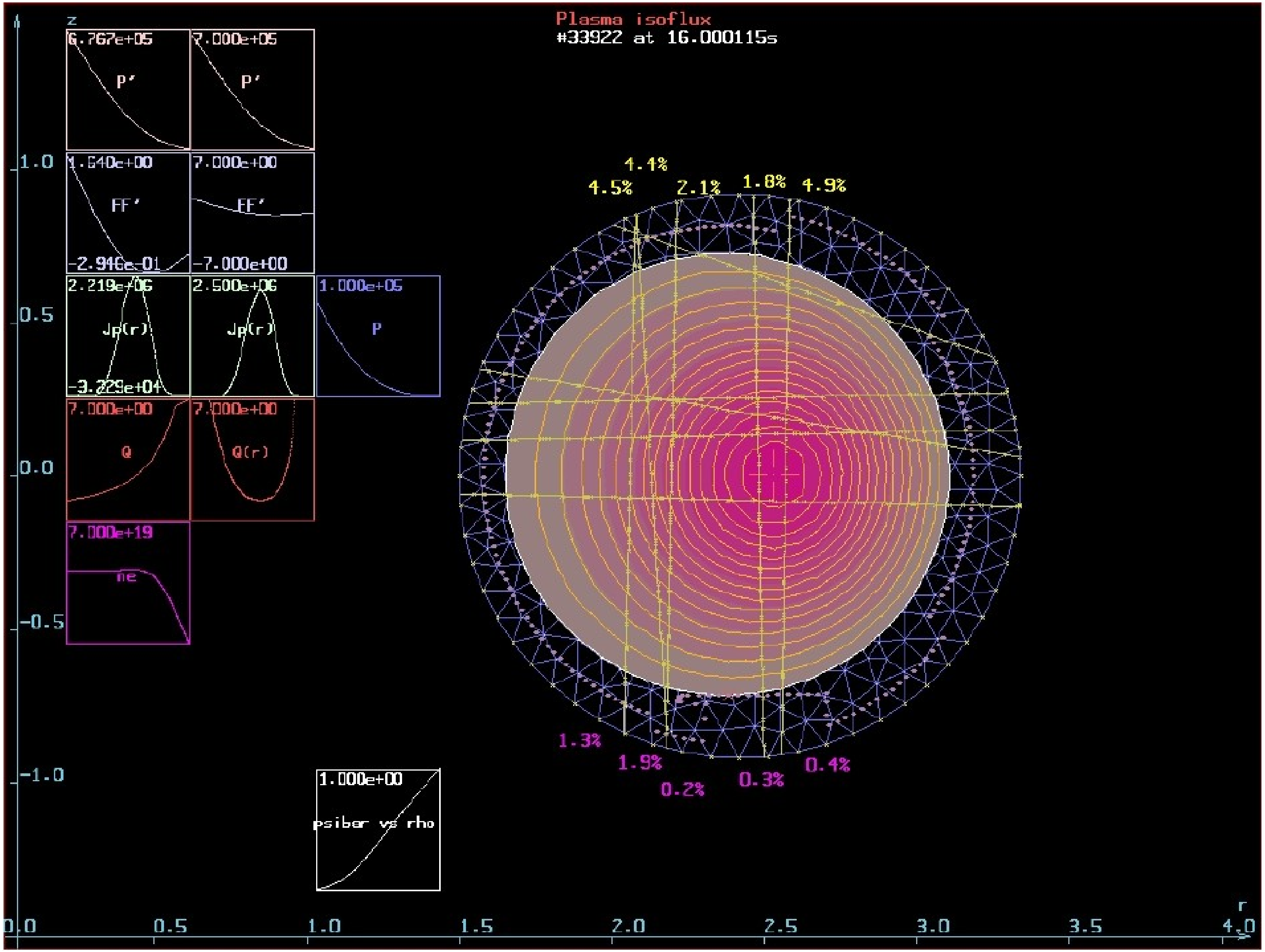

B. Faugeras, GT Plasma (2012)

Typical MHD equilibrium in Tore Supra

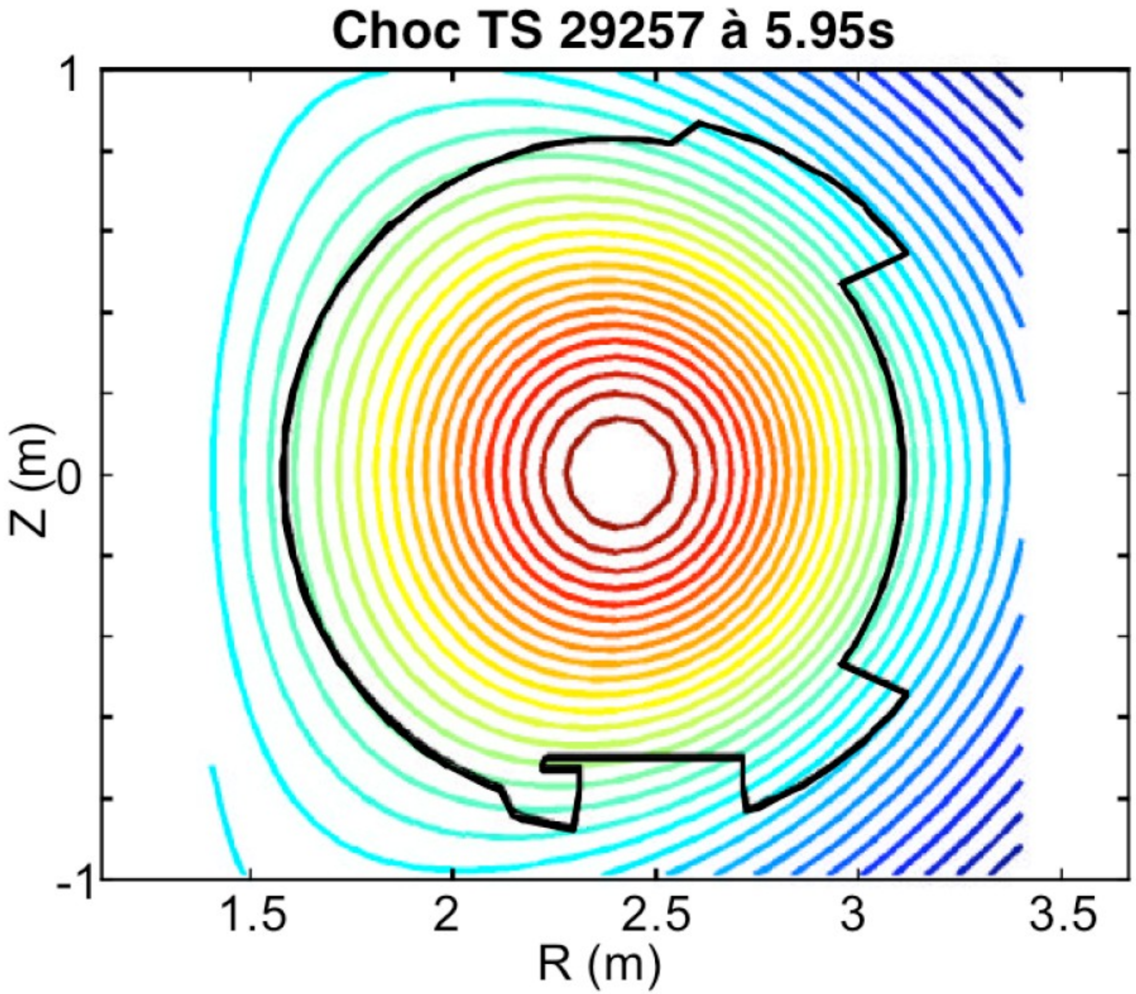

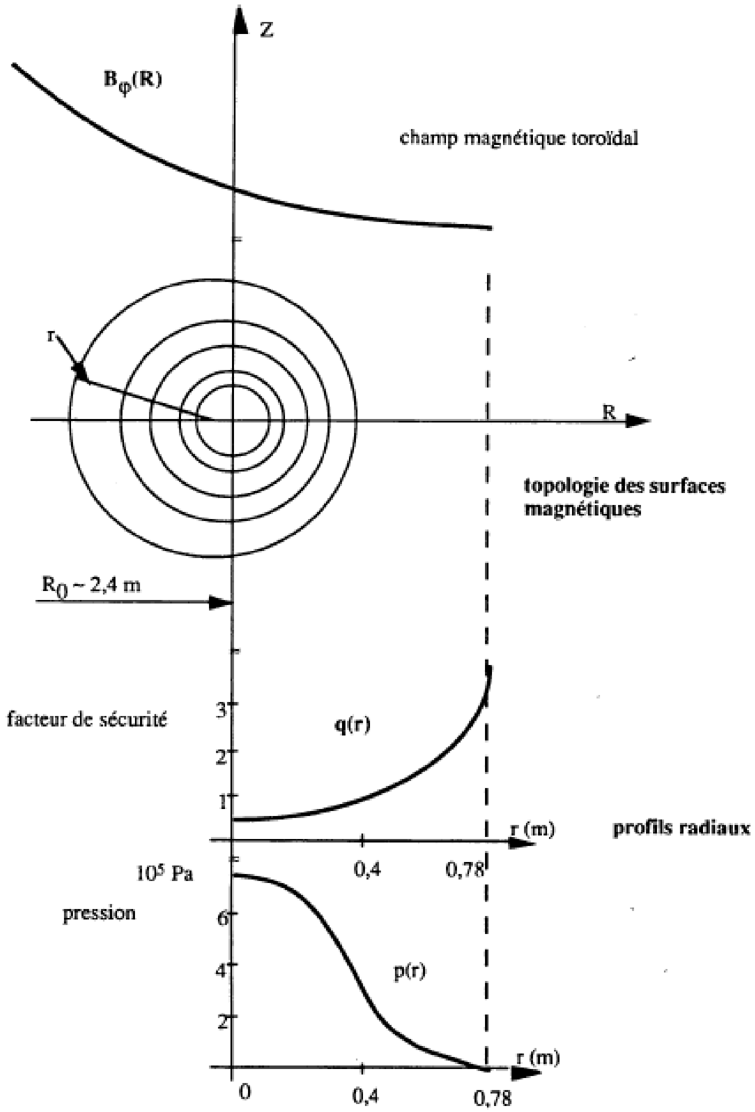

FIG. 1.6 – *Équilibre magnétique typique du tokamak Tore Supra.*

Any kind of magnetic configuration : Tore Supra

Pre-magnetization, maximum flux in the central coils, 40 kA, 8 Wb

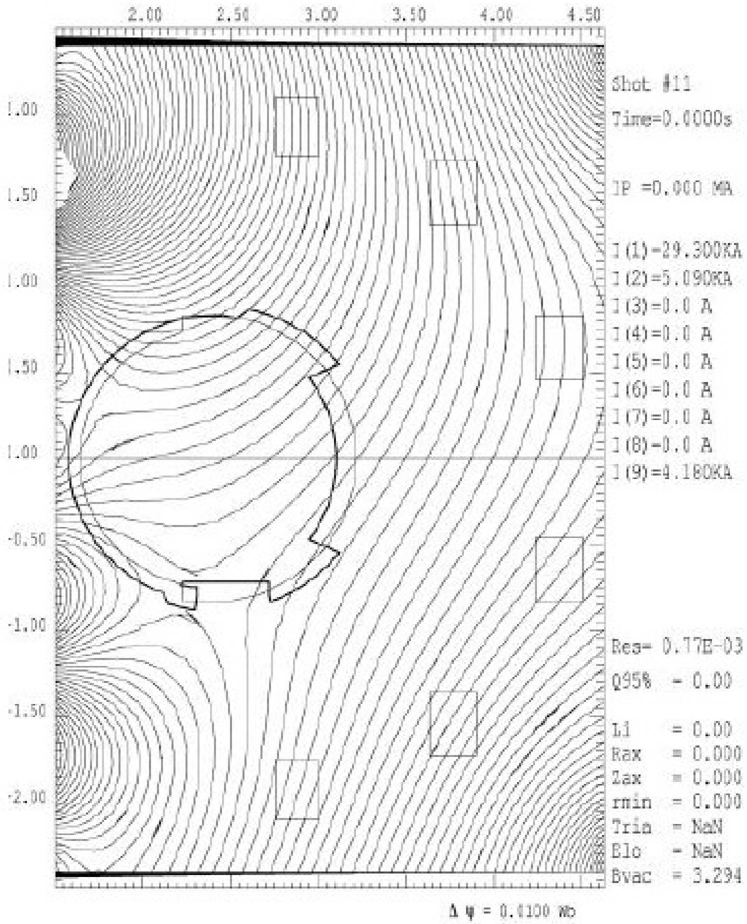

• **MAESTRO equilibrium :**

End of a disruption

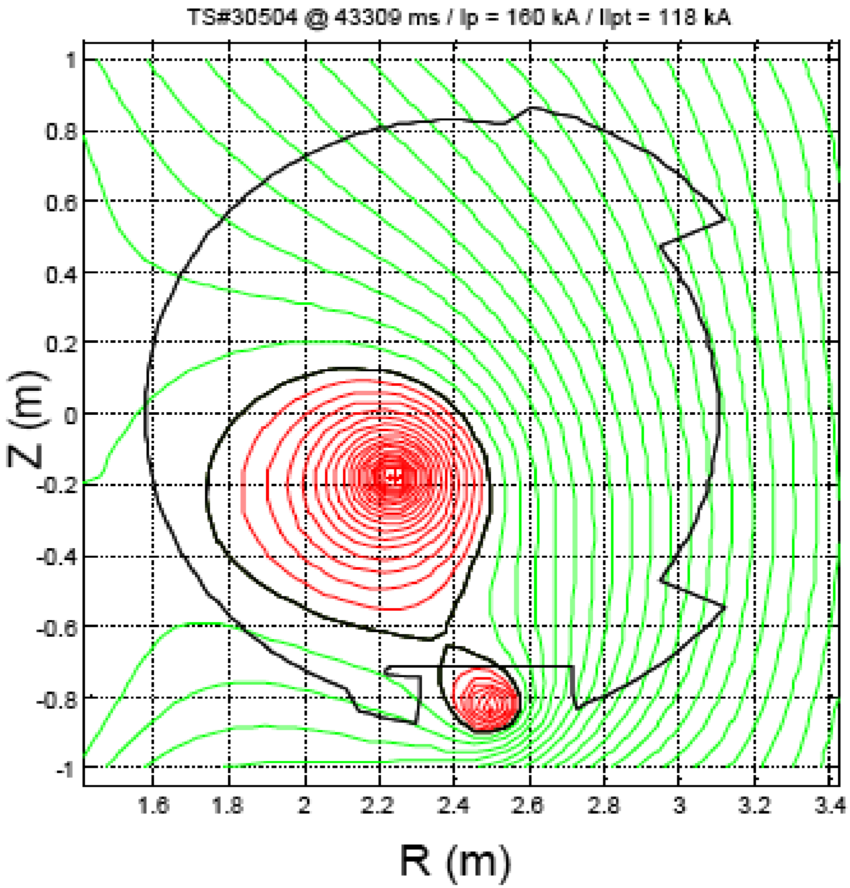

Equilibrium reconstruction : WEST

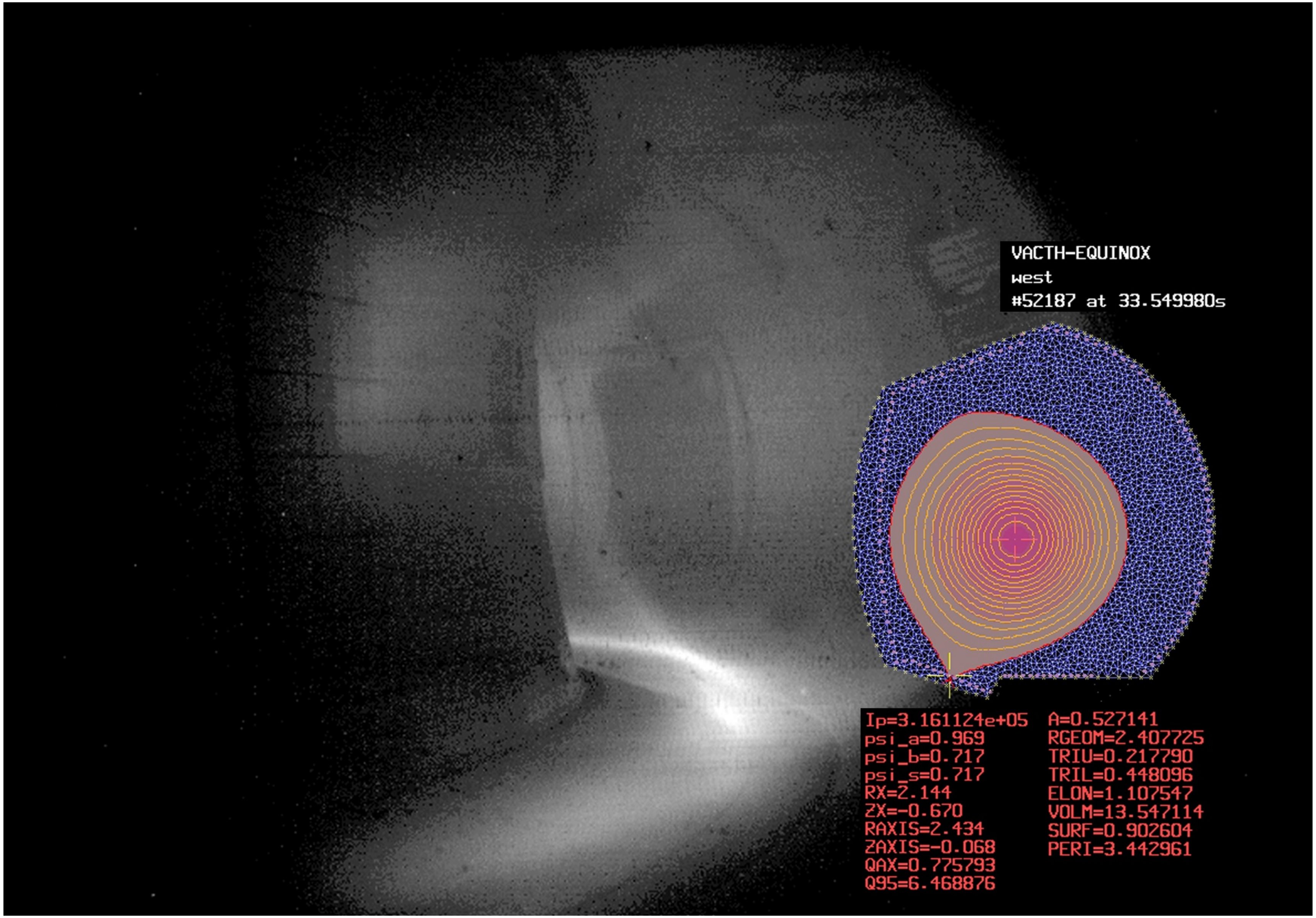

B. Faugeras, GT Plasma (2012)

Equilibrium real time control : Tore Supra

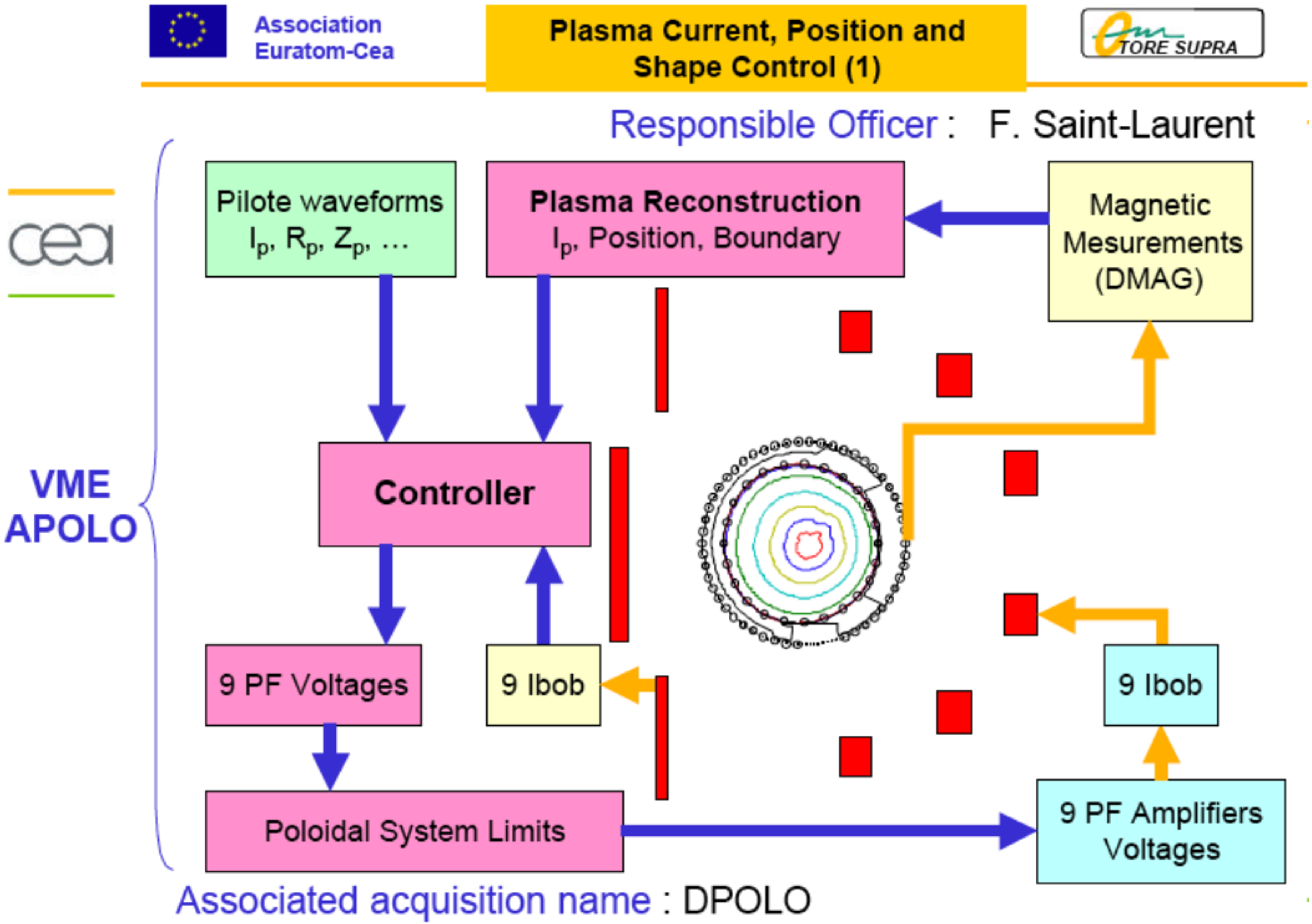

WEST plasma control

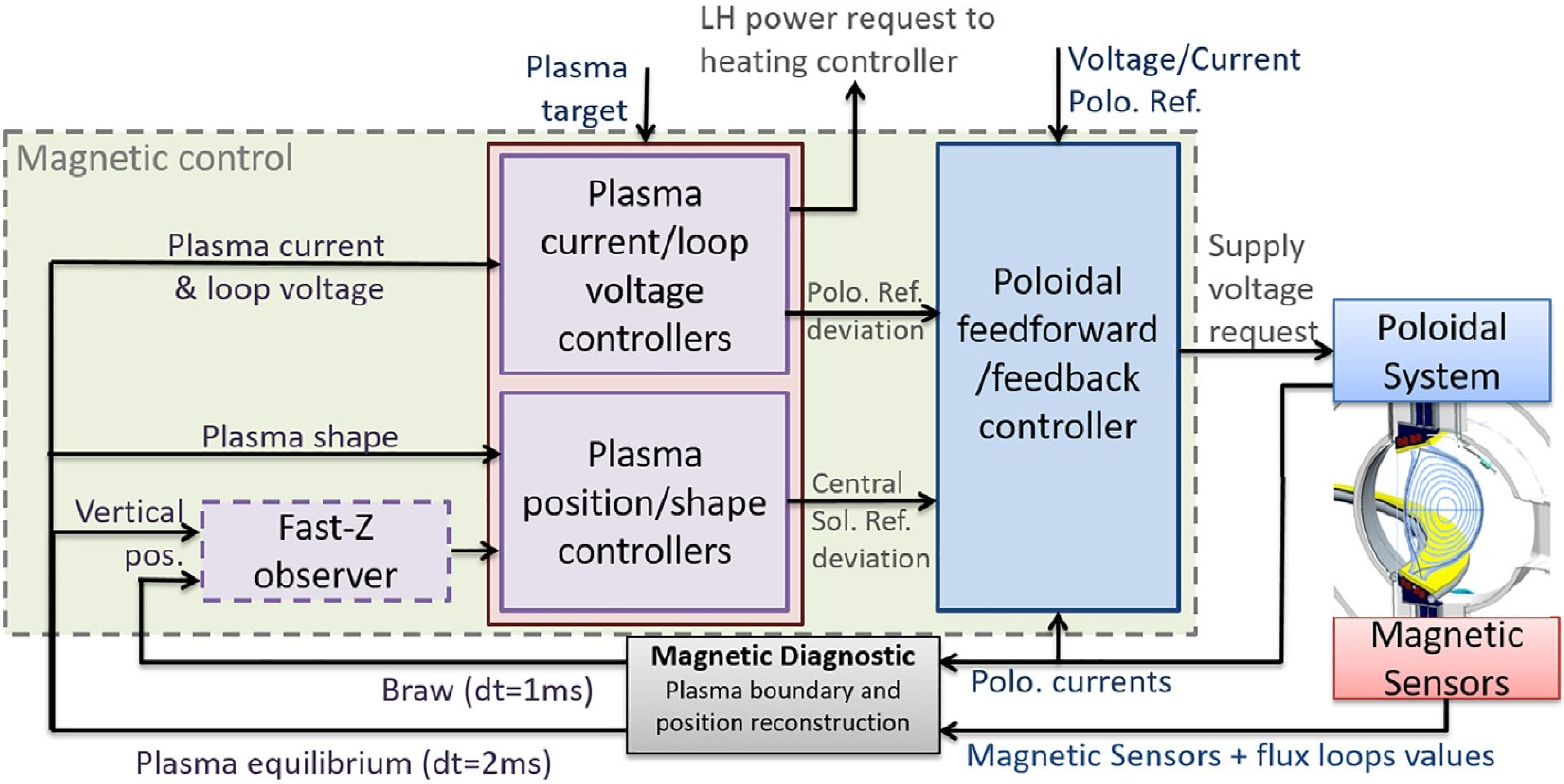

R. Nouailletas, Fus. Eng. Des. (2023)

Equilibrium reconstruction : JET

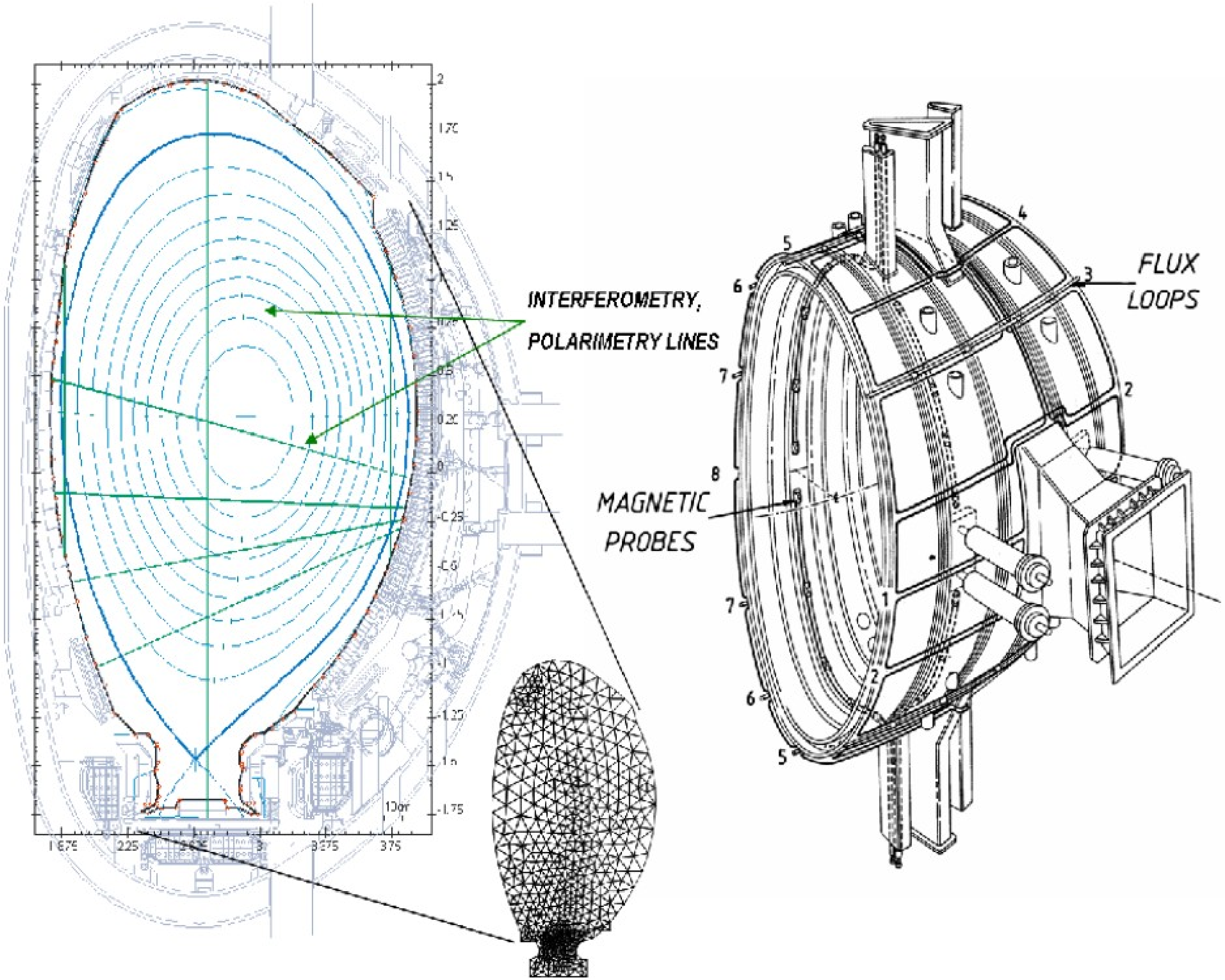

B. Faugeras, GT Plasma (2012), EQUINOX, real time equilibrium reconstruction

Equilibrium reconstruction : JET

With Polarimetry

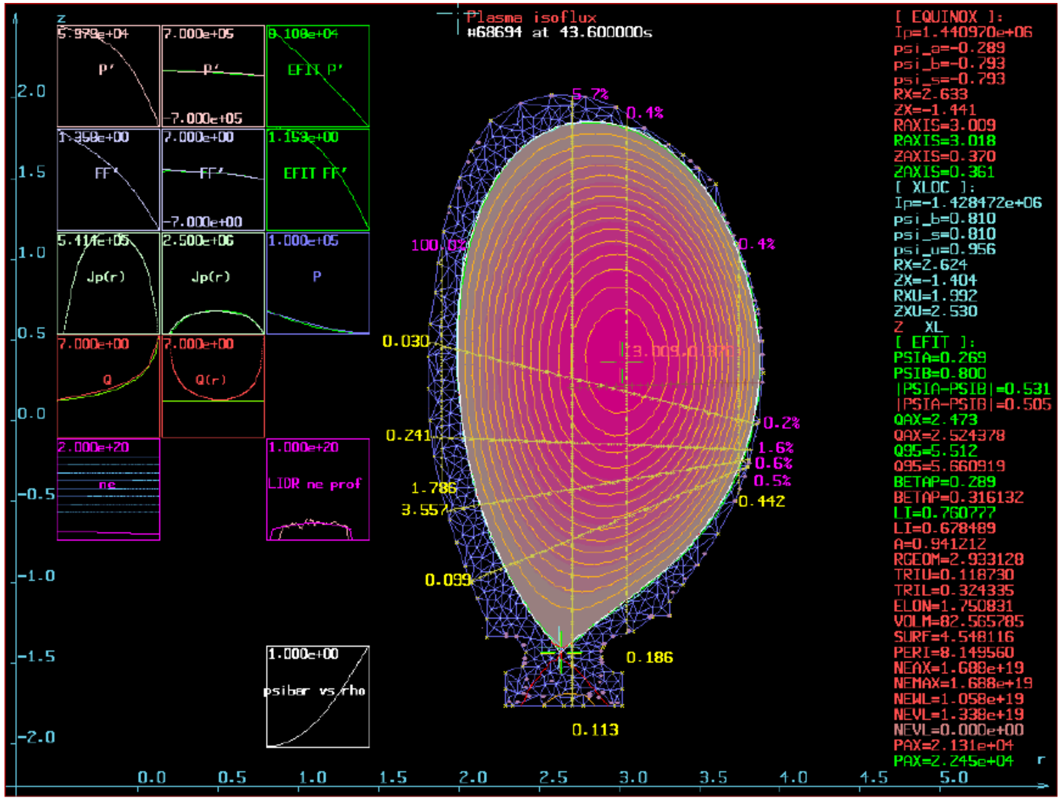

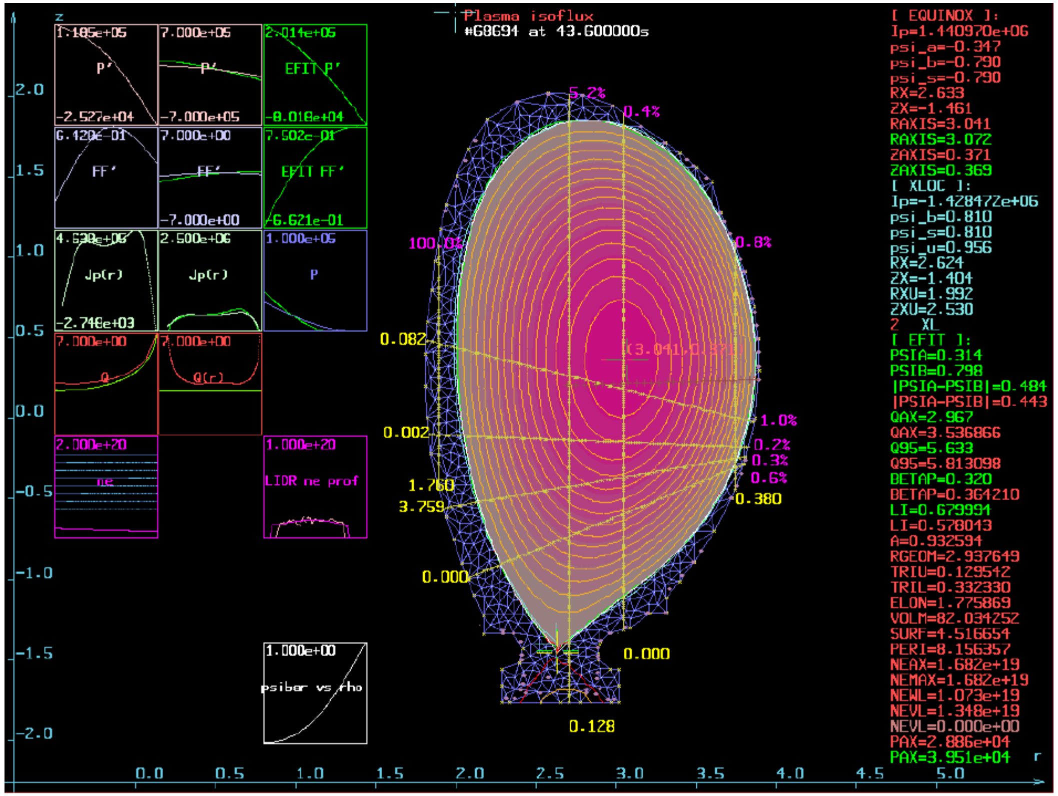

B. Faugeras, GT Plasma (2012)

Plasma shaping example : JT-60SA

The toroidal magnetic field is created by the coils with a poloidal shape (TF).

Le toroidal plasma current is induced in the plasma by the central solenoid (CS).

The plasma equilibrium and position are controlled actively by the EF coils (« Equilibrium Field »)
The fast control coil, are placed inside the chamber close to the plasma.

The plasma equilibrium is controlled passively by the stabilizing plates.

A X point divertor is placed in the lower part of the chamber.

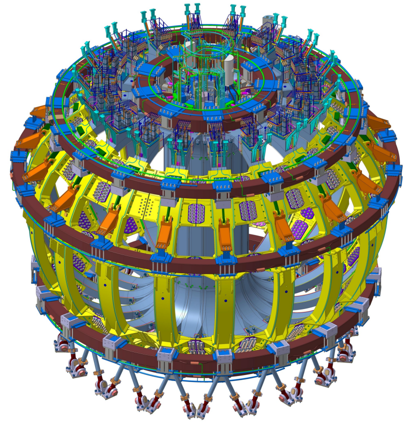

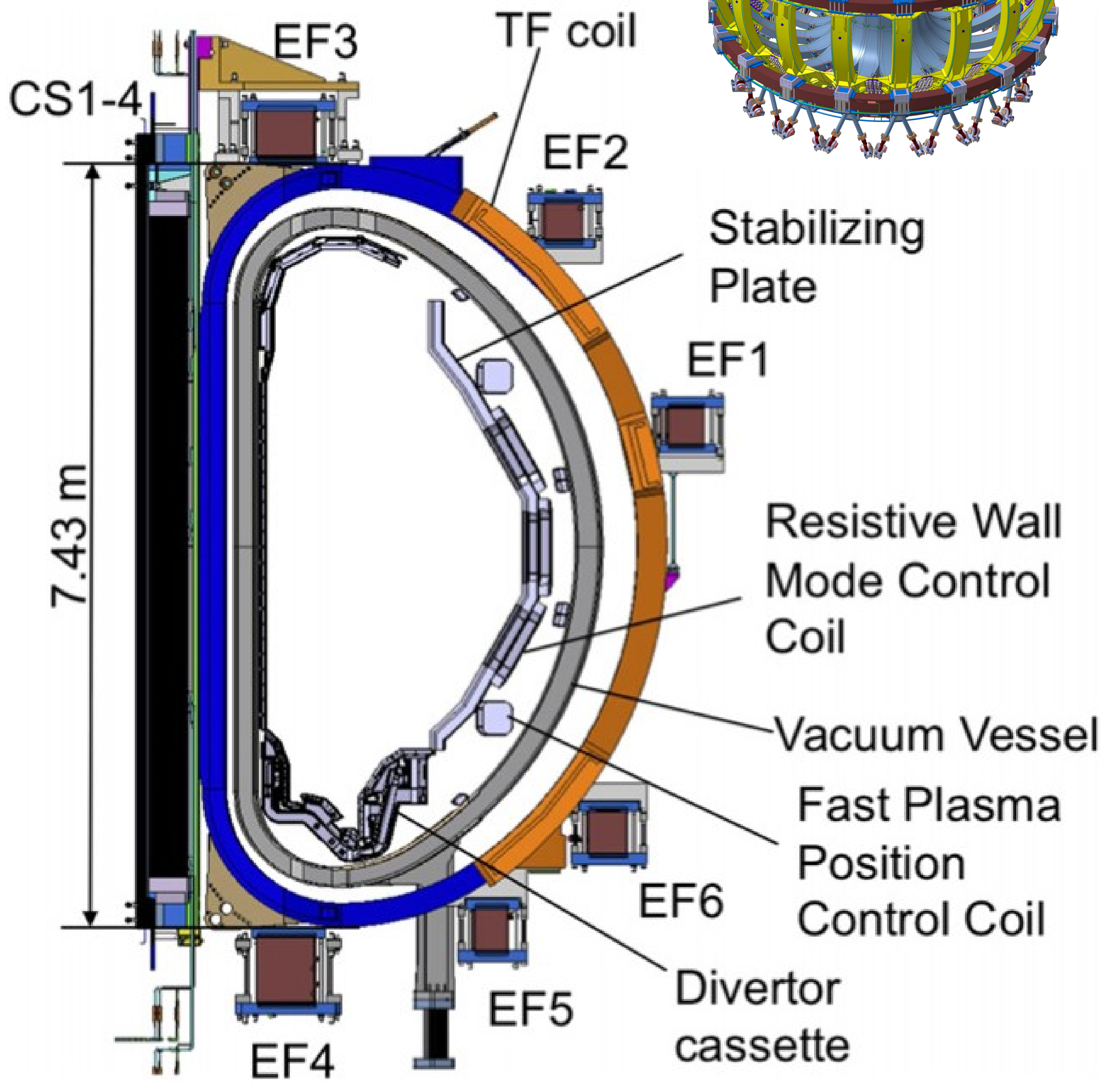

Bibliography

J. Wesson, Tokamaks, 3rd edition, Clarendon Press Oxford (2004)
Chap. 3 : Equilibrium
J. P. Freidberg, Plasma Physics and Fusion Energy, Cambridge Univ. Press (2008)
Chap. 11 : Macroscopic Equilibrium
W. M. Stacey, Fusion Plasma Physics, Wiley-Vch (2005)
Chap. 6 : Plasma equilibria
I. H. Hutchinson, Principles of Plasma Diagnostics, 2nd ed, Cambridge Univ. Press (2002)
Chap. 2 : Magnetic Diagnostics
Chap. 4 : Refractive-index Measurements
J.-M. Rax, Physique des Tokamaks, Éditions de l'École polytechnique (2011)
Chap. 7 : Magnétohydrodynamique
J. P. Goedbloed, R. Keppens & S. Poedts, Advanced Magnetohydrodynamics, Cambridge Univ. Press (2010)
Chap. 16 : Static equilibrium of toroidal plasmas
J. P. Goedbloed, R. Keppens & S. Poedts, Magnetohydrodynamics of Laboratory and astrophysical plasmas, Cambridge Univ. Press (2019)
Chap. 16 : Static equilibrium of toroidal plasmas

Physical constants

$k_B = 1{,}38\ 10^{-23} JK^{-1}$: Boltzmann constant
$h = 6.62\ 10^{-34} Js$: Planck constant
$C = 2{,}99\ 10^{8} ms^{-1}$: speed of light in vacuum
$\varepsilon_0 = 8.85\ 10^{-12} Fm^{-1}$: vacuum permittivity
$\mu_0 = 4\pi\ 10^{-7} Hm^{-1}$: vacuum permeability
$q_e = 1{,}60\ 10^{-19} C$: elementary charge
$m_e = 9{,}11\ 10^{-31} kg$: electron mass
$r_e = \frac{1}{4\pi\epsilon_0}\frac{q_e^2}{m_e C^2} = 2.82\ 10^{-15} m$: electron classical radius
$N_A = 6{,}022\ 10^{23} mol^{-1}$: Avogadro constant
$m_u = 1{,}66\ 10^{-27} kg$: atomic mass unit

- Standard parameters

$T_0 = 273.15 K$: standard air temperature $(0° C)$
$P_0 = 1{,}013\ 10^{5} Pa$: standard air pressure
$n_0 = 2{,}69\ 10^{25} m^{-3}$: ideal gas molecular density at T_0 and P_0

- Units

$1\,Torr = \frac{1{,}013\ 10^5}{760} Pa = 133{,}3\,Pa$: pressure corresponding 1 mm of mercury
$1\,eV = \frac{1{,}6\ 10^{-19}}{1{,}38\ 10^{-23}} K = 1{,}16\ 10^{4} K$